An insight into the breakup of Gondwana: Identifying events through low-temperature thermochronology from the basement rocks of Madagascar

Diane Seward

Geological Institute, Eidgenossische Technische Hochschule, Zurich, Switzerland

D. Grujic

Department of Earth Sciences, Dalhousie University, Halifax, Nova Scotia, Canada

G. Schreurs

Institute of Geological Sciences, University of Bern, Bern, Switzerland

Received 28 June 2003; revised 23 December 2003; accepted 25 March 2004; published 8 June 2004.

[1] Fission track analysis was applied to the Precambrian suites of Madagascar in order to identify the lower-temperature cooling histories and their relationships to the Phanerozoic events that affected the island. Apatite ages range from 431 to 68 Ma, and zircon ages range from 452 to 238 Ma. Thermochronologically, the island can be divided into a southern, central, and northern region each with a subdivision on an east-west basis. The southern region is sharply separated from the central region by strongly contrasting apparent apatite ages over the northwest-southeast striking Ranotsara Shear Zone (RSZ). The change in apparent ages over the RSZ is indicative of later reactivation along younger brittle faults. The central region has the oldest ages of the island and has a diffuse contact to the third region northward. Along the entire western margin of the Precambrian basement initial Paleozoic exhumation was followed by heating (burial by sediments) during Jurassic and Cretaceous times. A decrease in ages along the eastern margin from 119 to 68 Ma coincides with the predicted positions of the Marion hot spot after effects of erosion are considered. On the other hand, these ages may represent progressive opening of the margin in a southward direction together with associated denudation of the rift shoulder. The eastern part of the central region has remained very stable since at least Devonian times, undergoing only long-term very slow exhumation at rates of 1–5 m/Myr. *INDEX TERMS:* 1035 Geochemistry: Geochronology; 1099 Geochemistry: General or miscellaneous; 1206 Geodesy and Gravity: Crustal movements—interplate (8155); 8099 Structural Geology: General or miscellaneous; 8105 Tectonophysics: Continental margins and sedimentary basins (1212); *KEYWORDS:* thermochronology, passive margins, fission track, Gondwana. **Citation:** Seward, D., D. Grujic, and G. Schreurs (2004), An insight into the breakup of Gondwana: Identifying events through low-temperature thermochronology from the basement rocks of Madagascar, *Tectonics*, *23*, TC3007, doi:10.1029/2003TC001556.

0278-7407/04/2003TC001556

1. Introduction

[2] Madagascar is a key component in understanding the history of the break up of Gondwana. It was positioned between the present east African coast on the one side and the India-Seychelles block on the other before breakup (Figure 1). It was involved in an intra-continental rifting event during the late Paleozoic and subsequently in two major periods of ocean spreading at different times, affecting both the western and eastern margins separately. The drifting of the Madagascar-India-Seychelles-Australia-block from the east African region began at the latest at the time of the M25 anomaly, i.e., approximately 155 Ma [*Simpson et al.*, 1979; *Ségoufin and Patriat*, 1980; *Gradstein et al.*, 1994] and continued drifting southward until about 118 Ma. The India-Seychelles block broke away in the Late Cretaceous some time during the quiet magnetic period (A34, 118–84 Ma). Most studies in Madagascar until now have focused either on the tectonometamorphic evolution of the Precambrian of the interior region, or on the stratigraphy of the marginal basins. In the field of geochronology most work has previously concentrated on dating of Precambrian rocks and associated geological events as well as on the timing of Cretaceous volcanic extrusions. Little is known about the Phanerozoic thermal history of the Precambrian rocks, even though they formed the basement to the rift/drift-related sedimentary sequences. The lower temperature chronometers such as fission track analysis (FTA), which yield younger events that may not always be identified through either structural or stratigraphic analysis, have been attempted by *Seward et al.* [1998, 1999, 2000a] and *Emmel et al.* [2002]. Here we report on fission track analysis using the data sets to

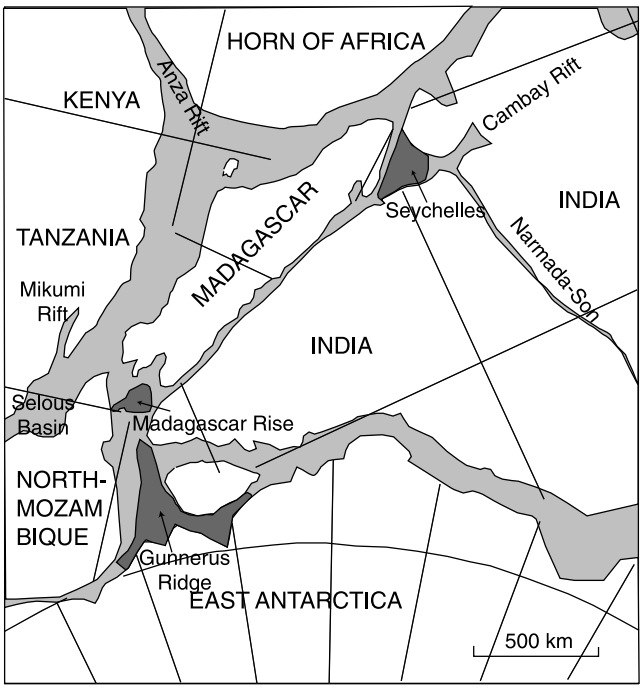

Figure 1. Reconstruction of Gondwana fragments at 200 Ma (modified from *Reeves et al.* [2002]). Open areas, geometrically rigid Precambrian crustal fragments; light shading, areas of originally continental rocks that have been extended and lost from outcrop by rifting; dark shading, largely submarine, partly Precambrian areas. Orthographic projection centered at 5°S, 45°E, African coordinates. (With permission from Elsevier Science.)

unravel the response of the Precambrian basement to Late Paleozoic and Mesozoic rifting and drifting.

2. Regional Setting

2.1. Plate Tectonic Setting and Regional History

[3] The island is essentially composed of a core of Precambrian basement with sedimentary basins on the western margin (Figures 2 and 3). The basement consists mostly of ortho- and para-metamorphic rocks and granitoids [*Besairie*, 1973]. Its structure is thought to have been the product of several tectonometamorphic events during the Archean and Neoproterozoic [e.g., *Andriamarofahatra et al.*, 1990; *Nicollet*, 1990; *Windley et al.*, 1994; *Paquette et al.*, 1994, 2003; *Kröner et al.*, 1996, 1999, 2000; *Paquette and Nédélec*, 1998; *Handke et al.*, 1999; *Tucker et al.*, 1999; *Collins*, 2000; *Martelat et al.*, 2000; *Nédélec et al.*, 2000; *de Wit et al.*, 2001; *Collins and Windley*, 2002; *Collins et al.*, 2003a, 2003b; *Fernandez and Schreurs*, 2003; *Fernandez et al.*, 2003; *de Wit*, 2003; *Goncalves et al.*, 2003; *Meert*, 2003]. These basement rocks have served as rift flanks during rifting and drifting since late Paleozoic times during the breakup of Gondwana. Intracontinental rifting began in the Upper Carboniferous with the development of half grabens which were filled with the fluvial and marginal marine sediments of the Sakoa and Lower and Middle Sakamena Formations [*Nichols and Daly*, 1989]. Clastic sedimentation of the Upper Sakamena Formation followed during the Middle Triassic. The Upper Triassic-Lower Jurassic sequence was dominated by fluvial sedimentation of the Isalo Formation deposited unconformably on the Upper Sakamena and overstepping onto the adjacent basement [*Clark*, 1998]. In the Bajocian (~176 Ma) regional marine conditions were initiated. This change in sedimentation represents the early stage of the formation of the Somali and Mozambique Basins.

2.1.1. Separation From Africa and Associated Development of the Western Basins

[4] At approximately 155 Ma, Madagascar (and the rest of East Gondwana) began to drift southward from Africa [*Reeves and de Wit*, 2000]. This was accompanied by the translation of Madagascar along a north-south trending transform fault located along the present Davie Ridge. By 140 Ma marine conditions prevailed in the developing marginal basins, i.e., the Diégo-Suarez, Mahajanga (Majunga) and Morondava basins [*Reeves and de Wit*, 2000].

[5] Much of the Lower Cretaceous corresponds to a period of very little deposition. Late Jurassic-Cretaceous faulting took place along the Precambrian and Paleozoic structures and was responsible for uplift, tilting and erosion [*Montenat et al.*, 1993, 1996]. Albo-Cenomanian clastic sediments rest unconformably on this eroded surface. By 118 Ma (M0) Madagascar had reached its present position and has moved little since, relative to Africa.

2.1.2. Separation From India-Seychelles

[6] The eastern margin of Madagascar became a rift shoulder during the separation of the Seychelles-India block. From the Late Cretaceous to the present, westward tilting in the Morondava Basin is coincident with this event [*Montenat et al.*, 1996]. The northeasterly drift of the Seychelles-Indian block from the eastern margin of Madagascar occurred somewhere in the period 118 and 84 Ma, on the basis of the oldest magnetic anomaly, A34. As the period A34 is the Cretaceous quiet magnetic zone, the time span is large, i.e., 34 Myr. It is possible to narrow the timing of separation down by using various other geological sources of evidence. On the basis of age determinations from palynology and sediment depositional rates in three wells on the western shelf of the Seychelles Plateau, *Plummer* [1996] suggested that the Seychelles microcontinent and Madagascar separated between 100 and 95 Ma. *Eldholm and Todal* [1997], who worked on the chronology of events in the Arabian Sea, placed the time of initiation of breakup between India-Seychelles and Madagascar at 100 Ma.

[7] Felsic volcanic subaerial rocks making up the St Mary islands, situated off the western coast of India, are thought to be related to the splitting of Madagascar and India-Seychelles. Whole rock K-Ar ages of 97.6 to 80.3 Ma [*Valsangkar et al.*, 1981] and a U-Pb zircon age of 91.2 ± 0.2 [*Torsvik et al.*, 2000] constrain the timing of this magmatism. The above studies then bracket the timing to between 100 and 80 Ma.

[8] During the Late Cretaceous, large volumes of basic lavas were extruded onto both the eastern and western

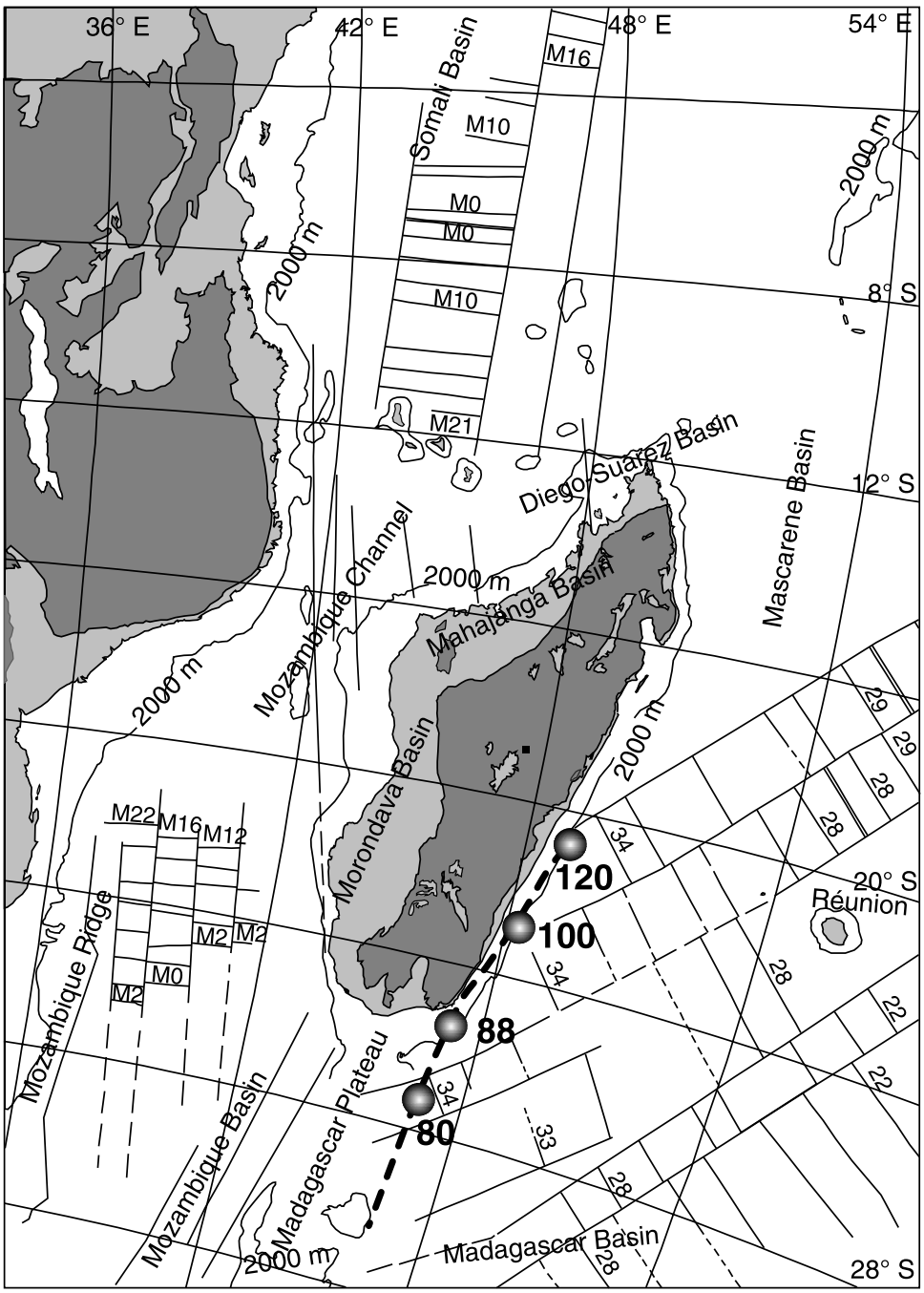

Figure 2. Current position of Madagascar with magnetic anomalies and transform ridges on the ocean floor (modified after *United Nations Educational, Scientific, and Cultural Organization* [1990]). Dark shading represents Precambrian rocks; light shading represents Phanerozoic rocks. Shaded circles are the positions and times proposed by *Storey et al.* [1995] and *Torsvik et al.* [1998] for Madagascar over the Marion hot spot.

coastal margins of Madagascar. On the basis of seventeen $^{40}Ar/^{39}Ar$ age determinations on volcanic rocks and dikes, a mean age of 87.6 ± 0.6 Ma was reported by *Storey et al.* [1995], who deduced that the duration of Cretaceous volcanism was no more than 6 Myr. Further, *Torsvik et al.* [1998], on the basis of a zircon-baddeleyite U/Pb age from northeast Madagascar of 91.6 ± 0.3 Ma and a $^{40}Ar/^{39}Ar$ age of 83.6 ± 1.6 Ma, estimated that the volcanism lasted a maximum 8 Myr. The volcanics are thought to be related to the position of Madagascar over the Marion hot spot, which in turn is considered to be associated with the breakup of India-Seychelles and Madagascar. On this basis, *Storey et*

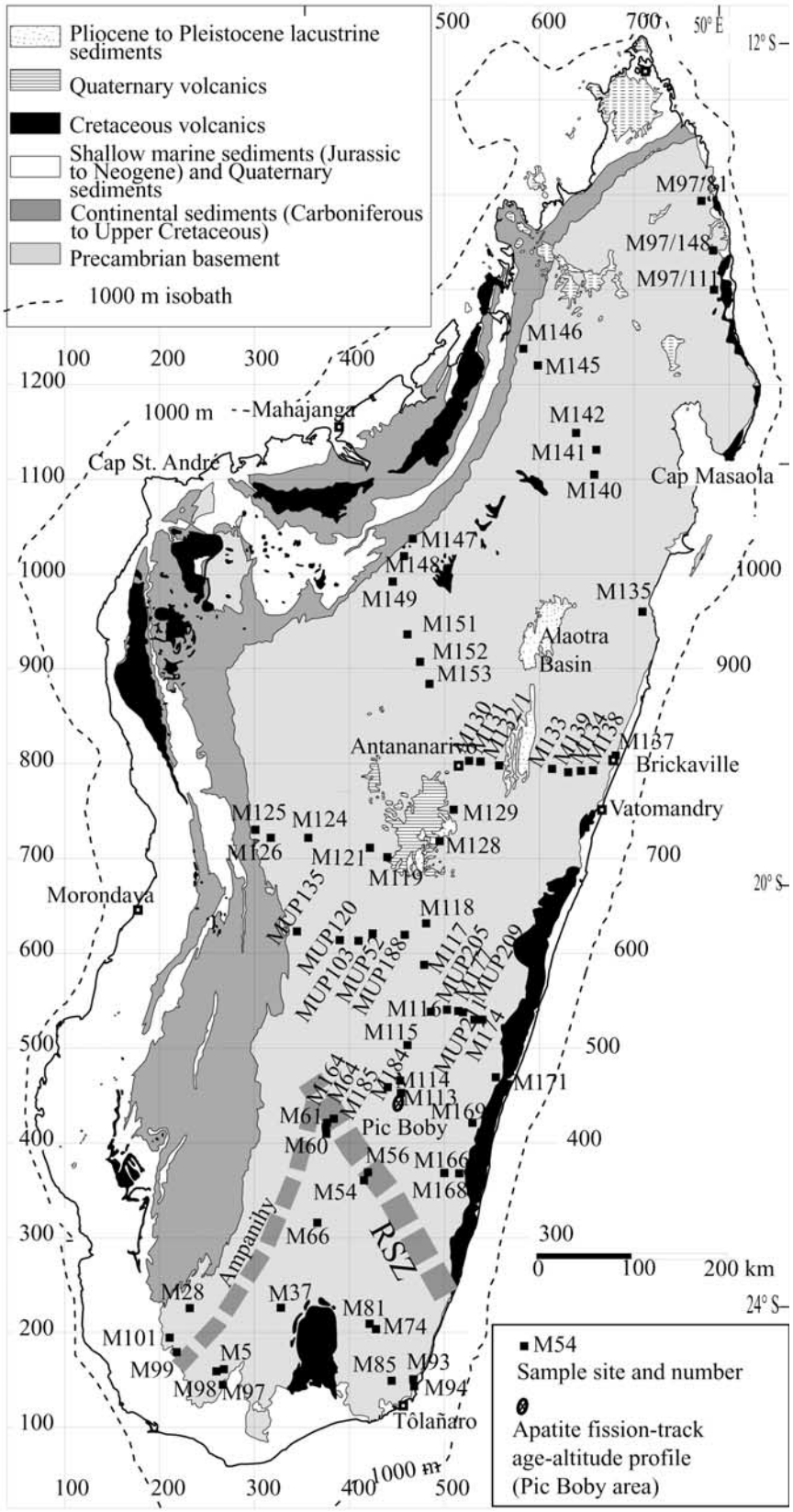

Figure 3. Simplified geological map of Madagascar [after *Besairie*, 1964] with location of samples. Grid lines are in Laborde projection.

al. [1995] placed the time of breakup at 88 Ma when they estimated that the southern tip of the eastern coast was over the Marion hot spot. *Storey et al.* [1995] argue that this is a case where the breakup was probably controlled by the participation of the mantle hot spot because of the close temporal and spatial coincidence with rifting. On the basis of paleomagnetic data, *Torsvik et al.* [1998] considered that the focal point of the Marion hot spot was beneath the central east coast at 118 Ma and at the south of Madagascar at circa 88 Ma (Figure 2). If the position and timing of the hot spot and drifting are interconnected then the separation may have extended over 30 Myr, perhaps propagating from north to south.

2.1.3. Post Breakup Tectonics

[9] Madagascar has been undergoing east-west extension [*Rakotondraompiana et al.*, 1999] since the middle Miocene and old north-south trending faults have been reactivated, often forming small sedimentary basins, e.g., the Alaotra Basin in the center of Madagascar (Figure 3). *Piqué et al.* [1999a] noted that Neogene to Quaternary sediments and volcanics tend to be associated with active faulting and extension. Brittle faulting and Neogene sediments [*Hottin*, 1976] in basins along the northwest - southeast striking Ranotsara Shear Zone (RSZ) suggests that this early Cambrian [*de Wit et al.*, 2001] ductile shear zone was also reactivated. Madagascar is seismically active, the seismicity being confined to the crust [*Rambolamanana et al.*, 1997]. The most frequent activity is in the central region and is often associated with major faults within the Neogene-Quaternary volcanic fields. The volcanism may be the cause of the higher altitudes in this region.

2.2. Geomorphology

[10] Madagascar has asymmetric relief. A steep eastern escarpment runs generally along and slightly oblique to the southern two thirds of the island at a distance of 10 to 125 km from the coast, (Figure 4a). The highest mountains reach almost to 3000 m. Rivers flowing eastward are short and cut steep gorges over the escarpment. A more gentle western slope has a well developed consequent drainage pattern directed away from the escarpment. In general the main east-west drainage divide lies 50–100 km from the eastern coast. However, there are two points where the divide is further inland, one immediately south of Antananarivo and the second just north of the RSZ.

[11] The Precambrian surface is dotted with granitoid inselbergs. Neogene to Quaternary volcanic landforms stand above the surrounding highlands.

3. Previous Geochronology

[12] In general, the geochronology of Madagascar has been restricted to studies of the greenschist to granulite facies Precambrian basement rocks or the Cretaceous volcanics. Most studies on the Precambrian basement have been done using the U/Pb methodology. A tonalite gneiss from Ile Sainte Marie dated at 3187 ± 2 Ma represents the oldest rock yet dated in Madagascar [*Tucker et al.*, 1999]. Late Archean intrusive igneous events at around 2530 to 2500 Ma have been identified throughout northern and central Madagascar [*Tucker et al.*, 1999; *Kröner et al.*, 2000; *Paquette et al.*, 2003]. U-Pb geochronology of other igneous rocks indicate voluminous and widespread magmatic activity (gabbroic and granitoid intrusions) in middle Neoproterozoic times at ~820–740 Ma in central and northern Madagascar [*Handke et al.*, 1999; *Kröner et al.*, 2000; *Tucker et al.*, 1999]. *Handke et al.* [1999] concluded that middle Neoproterozoic magmatism is related to Andean-type subduction of Mozambique oceanic lithosphere beneath central Madagascar, and *Fernandez et al.* [2003] argued that this magmatism is contemporaneous with the earliest deformation in the Itremo Group metasediments of central Madagascar, whereas *Collins et al.* [2003a] presented textural and metamorphic evidence that the ~800 Ma intrusions postdated early fabrics in the Itremo Group. Another important magmatic event occurred at ~630 Ma and corresponds to the emplacement of alkaline granites in northern central Madagascar [*Paquette and Nédélec*, 1998] and has been interpreted to represent post-collisional extension following the collision of Madagascar with East Africa at ~650 Ma [*Meert*, 2003; *Paquette and Nédélec*, 1998]. In contrast, *Collins et al.* [2003c] documented pervasive E-W shortening at granulite and upper amphibolite facies in central east Madagascar between 637 and 515 Ma. In southern Madagascar, *de Wit et al.* [2001] obtained U-Pb zircon and monazite ages in the 647–627 Ma range that were associated with early collisional events at granulite facies conditions, coeval with emplacement of anorthosites. Postcollisional events include localized deformation along prominent N-S striking shear zones at about 608 Ma, a period of slow cooling between 605 and 550 Ma, and accelerated exhumation at about 530–520 Ma [*de Wit et al.*, 2001]. In contrast, *Martelat et al.* [2000] on the basis of U-Th-Pb electron microprobe dating of monazites suggested that the earliest deformation and granulite facies metamorphism in southern Madagascar occurred at ~590–530 Ma and was followed by transpression at ~530–500 Ma resulting in refolding and formation of N-S striking shear zones. This timescale is supported by the depositional age of pre-collision metasediments in eastern Madagascar [*Collins et al.*, 2003b]. Late syntectonic to posttectonic alkaline magmatism at about 570 to 530 Ma occurs throughout central Madagascar [*Fernandez et al.*, 2003; *Handke et al.*, 1999; *Kröner et al.*, 2000; *Meert et al.*, 2001]. Th-U-Pb electron microprobe ages on monazites from metapelites of the Itremo Group in central Madagascar indicate monazite growth events in Paleozoic times at about 500 Ma and 430 Ma [*Fernandez et al.*, 2003]. These ages are also found in ^{40}Ar-^{39}Ar data and the ages have been interpreted as due to alteration related to fluid circulation events [*Fernandez et al.*, 2003].

[13] Other studies have involved the dating of the Cretaceous volcanics as mentioned above.

[14] *Seward et al.* [1998, 1999, 2000a] presented the initial results of the present study using apatite fission track analysis (AFTA). *Emmel et al.* [2002] using the same

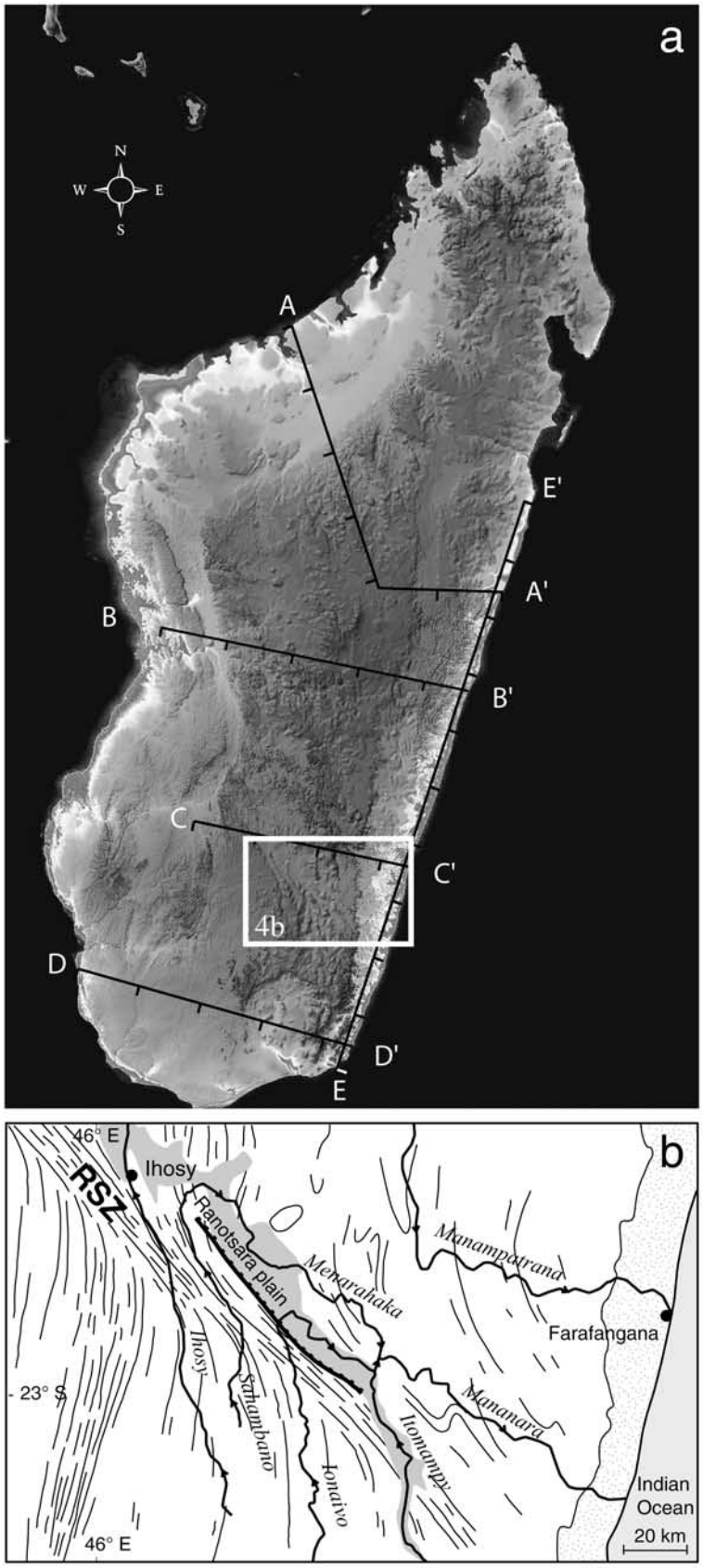
a
N
W
E
S
A
A'
B
B'
C
C'
D
D'
E
E'
4b
b
46° E
Ihosy
RSZ
Ranotsara plain
Menarahaka
Manampotrana
Farafangana
Ihosy
Sahambano
Ionaivo
Itomampy
Mananara
23° S
Indian
Ocean
20 km
46° E

Figure 4

method, made analyses on samples restricted to an area between latitude 17°–20° S, and obtained ages ranging from approximately 430 to 80 Ma displaying a general younging trend from west to east. They recognized enhanced cooling during the Carboniferous/Permian in the western region, which they related to the evolution of the eastern Morondava basin shoulder. Other localities, they concluded, were affected by the Cretaceous phase of rapid cooling reflecting the final breakup of Gondwana.

[15] The present contribution is based on apatite fission track analyses of the basement rocks extending across the entire island (Figure 3). Thermal modeling of the data sets (combining age and length parameters) was carried out for almost all samples. Only four zircon samples were dated due to the fact that most zircons were very metamict which causes the crystal surface to be too rough after etching for track identification. The data sets have been interpreted in terms of tectonic events, sedimentation history and landform development.

4. Fission Track Thermochronology

[16] For fission track systems, there are no discrete "closure" temperatures as in other radiogenic systems. A transition temperature zone where tracks are essentially unstable is recognized; this is termed the partial annealing zone (PAZ) and is defined by upper and lower temperature limits. However, an effective closure lies within these bounds, and is dependent on cooling rates. The PAZ for apatite lies between 60° and 120°C [*Laslett et al.*, 1987; *Corrigan*, 1993] with an effective closure temperature constrained at 100° ± 10°C. Hence apatite fission track analysis is particularly useful for evaluating low-temperature thermal histories, i.e., those affecting the upper 3–4 km of the crust.

[17] Research into zircon annealing is not as advanced as that for apatite; from experimental studies extrapolated to the geological timescale, current estimates for the partial annealing zone range are 390 to 170°C depending on the type of model used [*Yamada et al.*, 1995]. These authors defined the lower temperature limit as the temperature for 5% age reduction, whereas the upper limit is essentially total resetting to zero age. Many additional factors such as rates of cooling and chemical composition come into question. With a slow cooling rate and alpha damaged zircons we consider the effective closure temperature for zircons to be 240°C [*Brandon et al.*, 1998].

[18] Since fission tracks are produced continuously, each track in a sample will have been exposed to a different portion of the time and temperature history of its host rock and the distribution pattern of confined fission track lengths is an integrated cooling history. The time taken for a rock to pass through the partial annealing zone is reflected in the track length distribution. Further, if a sequence undergoes renewed burial and/or heating, preexisting tracks are shortened to a length determined by the maximum temperature and the duration of burial. At temperatures greater than the upper limit of the partial annealing zone, all tracks are erased and the "clock" is reset when the rock cools again through the partial annealing zone. Using the random Monte Carlo and Genetic Algorithm approach [*Gallagher*, 1995], the sample age and the track length parameters are compared to those determined through experimental annealing in order to assess some possible T-t paths.

[19] In this study, the paths were derived using no specific geological constraints; they were totally unconstrained and each sample was treated identically, i.e., with the same parameter space. An initial track length of 15.5 μm was used throughout, rather than 16.3 μm which underestimates track annealing and therefore overestimates cooling rates during the later stages (see discussion by *Gunnell et al.* [2003]). Every sample was treated in the same manner.

[20] The kinetics of annealing of the tracks has been found in some instances to be a function of chemical composition [e.g., *Gleadow and Duddy*, 1981; *O'Sullivan and Parrish*, 1995]. *Burtner et al.* [1994] have shown that this amounts to a variation in total annealing temperature by as much as ±20°C in extreme cases. The mean track pit diameter (1.8–2.0 μm) of the apatites in this study and electron microprobe analyses of selected samples suggests that the apatites are typically fluorapatites. Hence in modeling of T-t paths (using the "Monte Trax" software [*Gallagher*, 1995]), the annealing model of *Laslett et al.* [1987] for Durango apatite was used unless there were anomalous chemistries (see discussion in text).

5. Analytical Methods

[21] Sample preparation followed the routine separation techniques [*Seward*, 1989]. Etching of the apatites was done with 7% HNO_3 at 21°C for 55 s. This etch time yields identical track length parameters to the etch using 20 s in 5N HNO_3 [*Seward et al.*, 2000b] i.e., that used in the annealing studies by *Laslett et al.* [1987]. The zircons were etched in a eutectic mixture of KOH and NaOH at 220°C for between 20 and 32 hours. Muscovite detectors were etched in 40% HF for 50 minutes at room temperature. Irradiation was carried out at the ANSTO facility, Lucas Heights, Australia. Microscopic analysis was carried out using an optical microscope with a computer driven stage ("Langstage" software from *Dumitru* [1995]). All ages were determined using the zeta approach [*Hurford and Green*, 1983] with a zeta value of 355 ± 5 for CN5 and 119 ± 5 for CN1 (DS). They are reported as central ages [*Galbraith and Laslett*, 1993] with a 2σ error (Table 1). Where possible, 20 crystals of each sample were counted

Figure 4. (a) Shaded relief digital elevation model of Madagascar showing topography and location of cross sections mentioned in the text. The tick marks represent 100 km intervals equivalent to those on the sections in the text. (b) Drainage pattern diverted across the Ranotsara Shear Zone (RSZ).

Table 1. Fission Track Analyses From Precambrian Rocks of Madagascar[a]

Sample	Grid Reference	Altitude, m	Number of Grains Counted	Standard Track Density $\times 10^4$ cm^{-2} (Counted)	$\rho_s \times 10^4$ cm^{-2} (Counted)	$\rho_i \times 10^4$ cm^{-2} (Counted)	Mean Track Length, μm, Standard Deviation (Measured)	P(χ^2), % Variation	Age ± 2σ, Ma
*M5	S: 24°41′200 E:45°01′300	210	12	14.1 (1907)	2483 (1974)	244.1 (194)	...	9 (18)	238 ± 46
*M28	S: 24°06′300 E: 44°46′000	380	16	13.3 (1907)	1684 (2535)	95.7 (144)	...	34 (109)	384 ± 71
*M97/148	S: 13°58′30.9 E: 49°57′49.7	30	14	45.6 (2214)	1571 (4064)	91.6 (237)	...	46 (4)	452 ± 64
*M94	S: 24°50′042 E: 47°04′981	15	10	40.0 (3085)	164 (2117)	111 (143)	...	5 (22)	341 ± 76
M28	S: 24°06′300 E: 44°46′000	380	12	136 (3493)	174 (1301)	244 (1827)	13.04 ± 0.14 1.35 (100)	4 (20)	172 ± 15
M37	S: 24°06′000 E: 45°42′000	800	14	131 (3493)	383 (1468)	534 (2048)	12.33 ± 0.18 1.84 (100)	<1 (18)	167 ± 14
M54	S: 22°51′717 E: 46°34′957	530	20	106 (2844)	306 (1022)	320 (1068)	12.94 ± 0.15 1.48 (100)	56 (2)	181 ± 17
M56	S: 22°49′450 E: 46°35′676	570	20	140 (2900)	271 (1437)	177 (939)	12.32 ± 0.16 1.64 (100)	28 (6)	375 ± 36
M60	S: 22°24′884 E: 46°10′902	700	20	104 (2900)	348 (2340)	387 (2605)	11.93 ± 0.14 1.40 (100)	<1 (9)	166 ± 14
M61	S: 22°22′893 E: 46°11′013	690	20	132 (2900)	191 (1233)	176 (1134)	13.05 ± 0.17 1.45 (71)	96 (0)	254 ± 22
M64	S: 22°19′125 E: 46°14′947	670	20	114 (2900)	441 (1610)	334 (1219)	11.13 ± 0.20 2.07 (105)	<1 (15)	266 ± 34
M66	S: 23°17′750 E: 46°05′027	780	20	115 (2844)	531 (828)	333 (519)	12.92 ± 0.27 1.90 (48)	30 (7)	321 ± 40
M74	S: 24°18′473 E: 46°40′999	370	15	116 (2844)	225 (1559)	283 (1955)	13.08 ± 0.18 1.78 (100)	10 (9)	167 ± 16
M81	S: 24°15′336 E: 46°37′209	550	20	117 (2844)	482 (1730)	733 (2629)	12.15 ± 0.18 1.78 (102)	<1 (15)	144 ± 14
M85	S: 24°47′859 E: 46°51′745	80	18	112 (2844)	68.8 (755)	193 (2118)	13.65 ± 0.16 1.59 (100)	13 (10)	72 ± 7
M93	S: 24°47′791 E: 47°04′701	15	20	127 (2900)	53.2 (654)	180 (2206)	13.95 ± 0.17 1.69 (101)	3 (16)	68 ± 8
M94	S: 24°50′042 E: 47°04′981	15	20	135 (2900)	84.7 (651)	282 (2169)	13.25 ± 0.23 1.36 (34)	37 (5)	73 ± 7
M97	S: 24°49′562 E: 45°05′884	320	15	143 (2900)	257 (853)	306 (1018)	12.67 ± 0.19 1.66(79)	<1 (41)	221 ± 51
M98	S: 24°42′086 E: 45°02′092	260	20	120 (2900)	169 (1098)	192 (1245)	12.37 ± 0.16 1.61 (100)	99 (0)	187 ± 17
M99	S: 24°31′453 E: 44°37′299	240	19	109 (2900)	227 (1591)	310 (2166)	12.82 ± 0.14 1.00 (50)	<1 (15)	144 ± 15
M101	S: 24°22′735 E: 44°32′545	260	20	109 (2844)	132 (1650)	122 (1528)	10.85 ± 0.16 2.06 (169)	95 (0)	209 ± 16
M103	S: 22°11′863 E: 46°53′036	2658	20	157 (3576)	175 (1999)	139 (1597)	12.66 ± 0.23 1.59 (47)	10 (10)	341 ± 30
M104	S: 22°11′852 E: 46°53′311	2460	19	153 (3576)	219 (1640)	148 (1106)	12.65 ± 0.15 1.53 (100)	20 (7)	397 ± 36
M105	S: 22°11′852 E: 46°53′311	2460	10	149 (3576)	381 (1666)	347 (1517)	12.64 ± 0.15 1.5 (100)	13 (7)	289 ± 26
M106	S: 22°11′924 E: 46°53′717	2480	10	147 (3576)	393 (1229)	326 (1023)	11.90 ± 0.21 1.70 (63)	<5 (13)	312 ± 38
M107	S: 22°11′885 E: 46°53′969	2260	15	143 (3576)	382 (2445)	286 (1826)	12.22 ± 0.18 1.82 (100)	<1 (19)	342 ± 42
M108	S: 22°11′492 E: 46°54′244	2060	3	139 (3576)	171 (133)	200 (156)	11.97 ± 0.60 2.31 (15)	16 (9)	211 ± 55
M109	S: 22°09′141 E: 46°53′935	1990	10	138 (3576)	246 (662)	169 (454)	12.85 ± 0.63 1.98 (10)	48 (1)	351 ± 44
M110	S: 22°08′631 E: 46°53′733	1790	16	132 (3576)	226 (1142)	157 (795)	13.57 ± 0.14 1.52 (120)	99 (0)	332 ± 32
M112	S: 22°06′392 E: 46°54′799	1425	20	132 (3576)	227 (770)	231 (785)	13.00 ± 0.20 1.65 (69)	80 (0)	228 ± 24
M113	S: 22°03′442 E: 46°56′308	1230	8	130 (3576)	286 (418)	272 (397)	12.12 ± 0.39 1.50 (15)	5 (14)	235 ± 43
M114	S: 21°56′623 E: 47°55′769	930	20	128 (3576)	193 (826)	220 (939)	12.62 ± 0.18 1.75 (93)	35 (7)	201 ± 21
M115	S: 21°35′620 E: 47°00′164	930	12	139 (2903)	421 (2012)	422 (2018)	12.57 ± 0.18 1.66 (85)	<5 (10)	240 ± 22
M116	S: 21°17′224 E: 46°14′459	1340	20	136 (2903)	47.9 (448)	37.2 (348)	12.84 ± 0.16 1.63 (100)	98 (0)	308 ± 45
M117	S: 20°53′339 E: 47°10′269	1635	20	130 (2903)	55.1 (795)	50.0 (721)	12.54 ± 0.22 2.48 (124)	<5 (0)	253 ± 27
M118	S: 20°26′331 E: 47°11′230	1290	20	118 (2903)	!22 (610)	92.5 (462)	12.66 ± 0.16 1.61 (100)	94 (0)	274 ± 36
M119	S: 19°49′129 E: 46°47′734	1280	20	115 (2903)	327 (2864)	347 (3045)	12.02 ± 0.16 1.58 (102)	<1 (20)	194 ± 22
M121	S: 19°43′476 E: 46°37′377	980	14	106 (2903)	80.0 (509)	115 (732)	11.08 ± 0.23 1.69 (63)	<1 (36)	134 ± 30
M124	S: 19°37′872 E: 45°59′848	1020	20	96.7 (2903)	138 (779)	140 (790)	12.25 ± 0.15 1.35 (86)	38 (0)	169 ± 18
M125	S: 19°32′856 E: 45°28′103	270	16	93.7 (2903)	76.1 (695)	48.6 (444)	11.35 ± 0.35 1.97 (32)	53 (4)	255 ± 33
M126	S: 19°37′354 E: 45°37′182	660	10	128 (3040)	253 (750)	212 (625)	12.59 ± 0.16 1.27(65)	<1 (19)	267 ± 45
M128	S: 19°38′395 E: 47°18′520	1545	10	126 (3040)	169 (970)	186 (1068)	12.99 ± 0.18 1.62(79)	21 (7)	201 ± 22
M129	S: 19°21′299 E: 47°27′375	1475	12	124 (3040)	48.7 (304)	55.3 (345)	13.62 ± 0.28 1.63(33)	100 (0)	192 ± 31
M130	S: 18°53′728 E: 47°36′623	1270	20	122 (3040)	56.6 (685)	82.4 (997)	13.97 ± 0.14 1.45 (100)	6 (45)	150 ± 16
M131	S: 18°53′690 E: 47°43′373	1480	20	121 (3040)	314 (2861)	361 (3283)	12.88 ± 0.15 1.50 (100)	14 (0)	189 ± 16
M132	S: 18°55′960 E: 47°56′332	940	17	118 (3040)	76.7 (761)	82.1 (815)	12.39 ± 0.16 1.63 (100)	25 (0)	197 ± 16
M133	S: 18°57′468 E: 48°26′765	975	10	115 (3040)	138 (612)	257 (1141)	13.76 ± 0.17 1.23(54)	0 (22)	111 ± 20

Table 1. (continued)

Sample	Grid Reference	Altitude, m	Number of Grains Counted	Standard Track Density $\times 10^4$ cm^{-2} (Counted)	$\rho_s \times 10^4$ cm^{-2} (Counted)	$\rho_i \times 10^4$ cm^{-2} (Counted)	Mean Track Length, μm, Standard Deviation (Measured)	P(χ^2), % Variation	Age ± 2σ, Ma
M134	S: 18°58′427 E: 48°44′085	270	15	1.47 (3465)	88.2 (429)	285 (1385)	13.51 ± 0.31 1.81 (35)	<5 (33)	94 ± 21
M135	S: 17°26′873 E: 49°19′351	160	20	1.46 (3465)	64.5 (805)	143 (1787)	12.84 ± 0.24 1.79 (55)	<5 (27)	119 ± 18
M137	S: 18°49′573 E: 49°04′485	40	15	1.43 (3465)	145 (877)	444 (2694)	12.88 ± 0.18 1.78 (100)	<5 (24)	86 ± 14
M138	S: 19°57′878 E: 48°51′114	75	20	1.42 (3465)	27.7 (214)	72.8 (561)	14.30 ± 0.24 1.41 (34)	87 (87)	97 ± 16
M139	S: 18°59′108E: 48°36′264	470	19	1.38 (3465)	49.5 (332)	123 (828)	14.03 ± 0.17 1.36 (64)	13 (18)	101 ± 16
M140	S: 16°08′952 E: 48°49′788	450	10	136 (3465)	275 (857)	240 (748)	11.72 ± 0.33 2.32(50)	<1 (19)	278 ± 45
M141	S: 15°54′757 E: 48°50′366	335	20	1.34 (3465)	200 (1282)	201 (1286)	13.13 ± 0.14 1.31 (82)	22 (9)	235 ± 22
M142	S: 15°45′197 E: 48°38′879	310	10	133 (3465)	131 (452)	155 (533)	11.98 ± 0.19 1.94(101)	21 (11)	200 ± 31
M145	S: 15°06′637 E: 48°15′569	250	40	162 (2873)	168 (2104)	228 (2858)	12.51 ± 0.11 1.33 (144)	13 (13)	209 ± 16
M146	S: 14°57′404 E: 48°06′980	160	6	164 (2873)	151 (311)	185 (380)	12.07 ± 0.34 1.60 (22)	49 (49)	237 ± 37
M147	S: 16°46′103 E: 47°01′937	30	20	158 (2873)	69.3 (787)	56.8 (645)	12.36 ± 0.11 1.14 (100)	50 (5)	337 ± 40
M148	S: 16°56′462 E: 46°56′992	100	6	156 (2873)	129 (487)	125 (473)	11.7 ± 0.30 1.70 (33)	<5 (21)	298 ± 66
M149	S: 17°11′170 E: 46°50′686	160	16	155 (2873)	113 (530)	145 (680)	12.51 ± 0.19 1.46 (62)	<5 (27)	205 ± 32
M151	S: 17°41′154 E: 46°59′028	715	10	152 (2873)	222 (749)	321 (1081)	12.84 ± 0.18 1.82 (101)	91 (0)	187 ± 20
M152	S: 17°57′017 E: 47°07′036	1491	20	151 (2873)	248 (2334)	252 (2372)	13.36 ± 0.16 1.57 (100)	<5 (14)	262 ± 25
M164	S: 22°21′702 E: 46°11′619	710	8	171 (3860)	117 (273)	129 (303)	11.68 ± 0.75 2.26(9)	82 (0)	268 ± 46
M166	S: 22°49′098 E: 47°23′443	200	14	180 (2332)	234 (601)	226 (579)	11.80 ± 0.29 2.21 (59)	6 (20)	325 ± 42
M168	S: 22°48′172 E: 47°34′855	95	18	132 (3491)	110 (1043)	63.2 (600)	12.88 ± 0.17 1.67(100)	22 (65)	396 ± 44
M169a	S: 22°20′359 E: 47°40′743	45	20	156 (3491)	122 (1148)	95.4 (899)	12.94 ± 0.32 2.26(51)	<5 (18)	350 ± 45
M171	S: 21°54′218 E: 47°31′772	75	20	138 (3491)	32.5 (389)	76.4 (916)	. . .	73 (0)	103 ± 13
M174	S: 21°20′869 E: 47°44′108	200	20	147 (3491)	191 (1571)	111 (914)	13.87 ± 0.19 1.42(59)	12 (12)	431 ± 46
M177	S: 21°16′759 E: 47°31′772	600	10	144 (3491)	90.3 (1410)	683 (1066)	11.17 ± 0.23 1.70(56)	39 (3)	331 ± 30
M182	S: 22°09′335 E: 46°53′984	1020	20	135 (3491)	69.1 (568)	71.2 (585)	13.08 ± 0.22 1.86(69)	20 (13)	231 ± 32
M184	S: 22°11′574 E: 46°54′063	2115	17	150 (3491)	352 (1624)	322 (1489)	12.93 ± 0.20 1.73(73)	33 (8)	283 ± 25
M185	S: 22°00′162 E: 46°48′664	2375	11	123 (3491)	156 (1041)	117 (780)	11.85 ± 0.32 2.43 (59)	20 (0)	287 ± 57
MUP52	S: 20°32′050 E: 46°38′650	1175	19	191 (3077)	67.1 (622)	47.4 (439)	12.38 ± 0.30 1.77(35)	70 (0)	292 ± 38
MUP103	S: 20°32′300 E: 46°29′950	1490	5	127 (3077)	384 (163)	250 (106)	11.91 ± 0.31 2.30(56)	52 (<1)	339 ± 85
MUP120	S: 20°31′100 E: 45°52′800	1150	20	116 (3077)	218 (1735)	199 (1584)	10.10 ± 0.22 2.38 (114)	<5 (18)	221 ± 25
MUP135	S: 20°36′000 E: 46°19′100	1225	20	136 (3077)	247 (2047)	249 (2063)	12.49 ± 0.24 1.48(38)	<5 (14)	238 ± 22
MUP188	S: 20°33′100 E: 46°58′350	1400	10	133 (3077)	395 (900)	302 (688)	13.25 ± 0.15 1.56(105)	79 (0)	301 ± 32
MUP205	S: 21°15′700 E: 47°24′100	1050	10	133 (3000)	296 (1249)	220 (927)	12.56 ± 0.18 1.79(100)	<1 (16)	316 ± 46
MUP209	S: 21°17′200 E: 47°33′800	600	12	130 (3000)	318 (1556)	220 (1079)	11.33 ± 0.26 1.81(47)	10 (10)	322 ± 34
MUP211	S: 21°21′100 E: 47°41′100	500	20	114 (3077)	137 ()1482)	101 (1089)	12.01 ± 0.16 1.62(100)	5 (13)	271 ± 29
M97/81	S: 13°31′32.9 E: 49°49′57.6	300	10	108 (3076)	150 (516)	203 (696)	13.45 ± 0.20 1.56(63)	15 (10)	141 ± 20
M97/111	S: 14°22′10.4 E: 49°58′20.1	300	10	117 (3076)	186 (378)	375 (760)	12.68 ± 0.19 1.72(82)	32 (15)	103 ± 14
M97/148	S: 13°58′30.9 E: 49°57′49.7	30	11	111 (3076)	278 (685)	352 (867)	11.72 ± 0.03 1.91(40)	79 (<1)	154 ± 17

[a]Asterisk represents zircon samples. The ρ_s and ρ_i represent sample spontaneous and induced track densities; P(χ^2) is the probability of χ^2 for v degrees of freedom where v equals number crystals −1. All ages are central ages [*Galbraith and Laslett*, 1993]. Here $\gamma_D = 1.55125 \times 10^{-10}$. A geometry factor of 0.5 was used. Zeta = 355 ± 5 for CN5/apatite and 119 ± 5 for CN1/zircon. Irradiations were performed at the ANSTO facility, Lucas Heights, Australia.

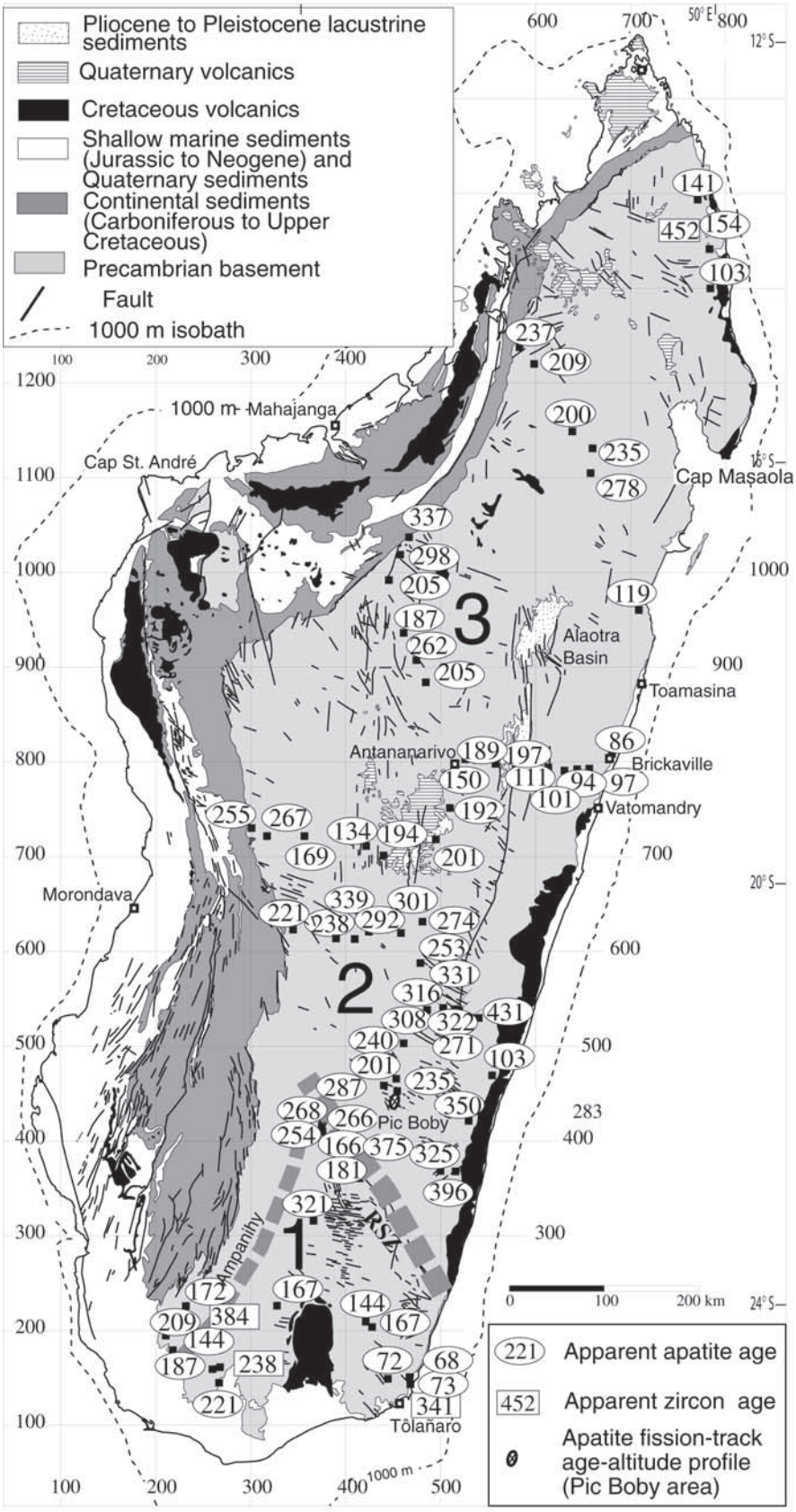
Pliocene to Pleistocene lacustrine sediments
Quaternary volcanics
Cretaceous volcanics
Shallow marine sediments (Jurassic to Neogene) and Quaternary sediments
Continental sediments (Carboniferous to Upper Cretaceous)
Precambrian basement
Fault
1000 m isobath
Mahajanga
Cap St. André
Cap Masaola
Alaotra Basin
Toamasina
Antananarivo
Brickaville
Vatomandry
Morondava
Pic Boby
Ampanihy
Tôlañaro
RS4
1
2
3
0 100 200 km
Apparent apatite age
Apparent zircon age
Apatite fission-track age-altitude profile (Pic Boby area)

Figure 5

for age determination. The magnification used was x1250 for apatite and x1600 oil for zircon. Horizontal confined track lengths in apatite were measured at x1250.

6. Results and Interpretation

[22] Apatite ages in the Precambrian basement rocks of Madagascar range from 431 ± 46 to 68 ± 8 Ma (Figure 5) with track lengths ranging from 10.85 μm to 13.95 μm (Table 1). In general as mentioned above, zircons were unsuitable for analysis but the four ages obtained range from 452 ± 64 to 238 ± 46 Ma. Unless stated, the following discussion is based on the results from the apatite analysis.

[23] Such a wide range of ages is to be expected from samples covering a vast region with a long history. Because the track lengths are relatively short in general, these are apparent ages and in themselves do not reflect per se a single cooling event. However, as a first order exercise, it is clear that the ages fall into three geographical groupings:

[24] 1. South of the RSZ the ages are in general younger than 238 Ma excluding one older sample, (region 1, Figure 5 and Table 1) which has an apparent age of 321 ± 40 Ma. This sample however, has a peculiar chemistry relative to other samples, with a chlorine content of 1%wt which has resulted in the preservation of the older age [*Green et al.*, 1989] and is considered regionally nonrepresentative. Ages reveal a younging trend from west to east (Figure 5).

[25] 2. North of this shear zone and stretching to about latitude 20°S, ages are older (region 2, Figure 5) ranging from an anomalously young 103 Ma to 431 Ma. The northern limit is not clear because of the rather poor distribution of samples. Within this grouping the apparent age trend is opposite to the southern one, with a gradation from older ages in the east to younger in the west with one exception, that of 103 Ma, located on the eastern coastal plain. This latter age will be discussed later, as it is not representative of this region.

[26] 3. North of the central region, ages tend to be younger and are rather mixed, ranging from 337 to 86 Ma (region 3, Figure 5), however, there is a general decrease from the western basin margins to the east coast. This is similar to the results determined by *Emmel et al.* [2002] for part of this region. We were unable to incorporate the data sets of *Emmel et al.* [2002] because the detailed positions are not available.

[27] A further overview reveals that the youngest ages of the island lie along the eastern margin of the northern and southern blocks with a general trend of younging within this subgroup from north to south.

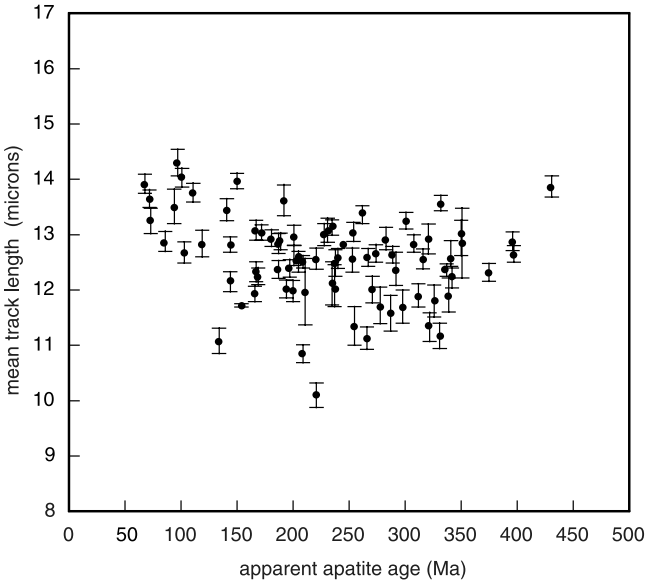

Figure 6. Correlation of apparent apatite age and mean track length.

[28] This raw data set implies on a first order inspection that the eastern central region has been undergoing cooling for a longer period than its north and south neighbors. The jump to younger ages south of the RSZ suggests that the southern region was exhumed, most likely along brittle faults which had developed within the shear zone. The abrupt termination of the subaerial Cretaceous volcanics along the east coast at the southeastern tip of the RSZ also supports the idea of an uplifted southern block along this structure. The age of the volcanics (≈88 Ma [*Storey et al.*, 1995]) suggests that the uplift may have been ongoing at least until this time.

[29] A further preliminary assessment of the data, is seen through the relationship of mean track length and age. Long track lengths imply a period of rapid cooling, often interpreted in terms of an event. The longest track lengths correlate to ages at approximately 430 Ma and 100–75 Ma (Figure 6). The younger is associated with the exhumation of rocks that either may have been reset during the passage of Madagascar over the Marion hot spot and/or represent cooling of the uplifted shoulder during separation of the India-Seychelles block from Madagascar.

6.1. Age-Altitude Relationship

[30] The relationship of age with altitude for the whole set of data (Figure 7) reveals only a very broad positive correlation. This plot is similar to those recognized in

Figure 5. Simplified geological map of Madagascar [after *Besairie*, 1964] showing apparent fission track ages (Ma). Grid lines are in Laborde projection. Faults in the basement are interpreted from Landsat TM images. Faults in sedimentary basins are mainly after *Montenat et al.* [1993, 1996], *Bertil and Regnoult* [1998], *Wescott and Diggins* [1998] and *Razafindrazaka et al.* [1999].

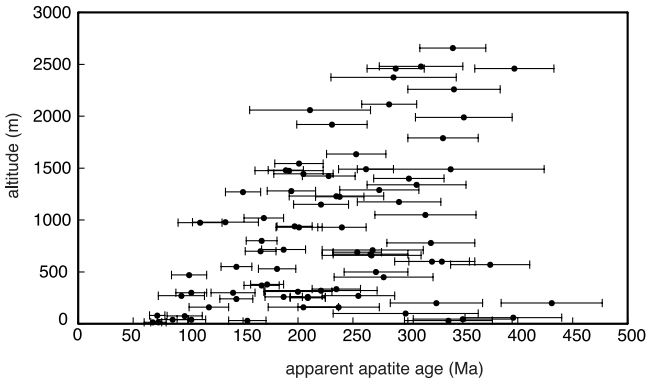

Figure 7. Age-altitude relationship of basement samples from Madagascar (errors are 2 sigma).

other fission track studies of passive margin regions (e.g., Namibia [*Brown et al.*, 1994], eastern Brazil margin [*Gallagher et al.*, 1995], western India [*Gunnell and Fleitout*, 1998]). The wide variation in apparent ages results from a number of diverse processes and can be interpreted in various ways. Diverse regional tectonic activity, variable erosion rates, variable chemistry and associated variability in the kinetics of cooling of the apatites as well as post closure-temperature movement taking rocks away from their original position after cooling, can all affect the age pattern. A breakdown into the three different geological regions discussed above, did not bring about clear trends except for two sections. A vertical section through Pic Boby (Figures 3 and 8a) revealed age differences separated by as much as 100 Ma at similar altitudes. Initially these were interpreted as being due to lithologic and/or possible chemical variations [*Seward et al.*, 1999], however, all these samples have since been chemically analyzed under the electron microprobe and no clear differences could be identified. All are fluorapatites and no real or systematic variation was found in any component. Field evidence for faulting was not found

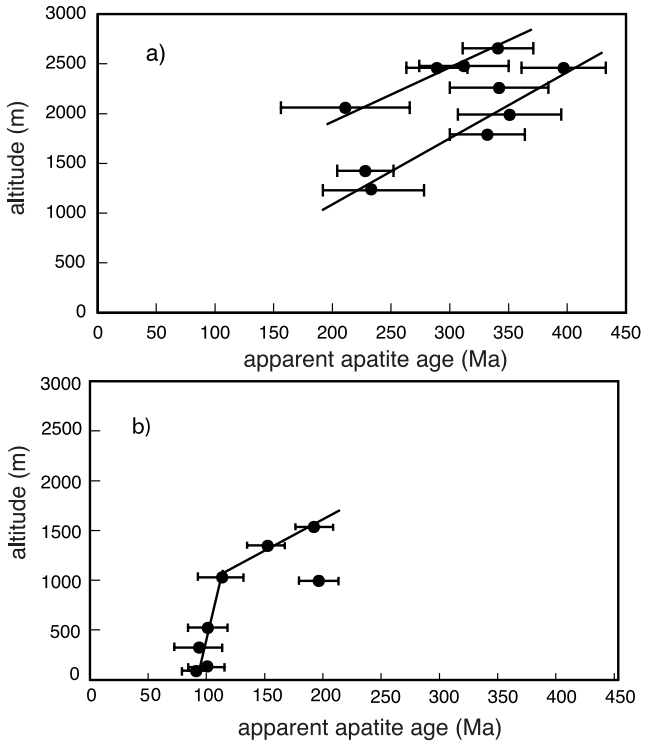

Figure 8. Age-altitude relationship of selected regions: (a) Pic Boby and (b) east from Brickaville to Antananarivo.

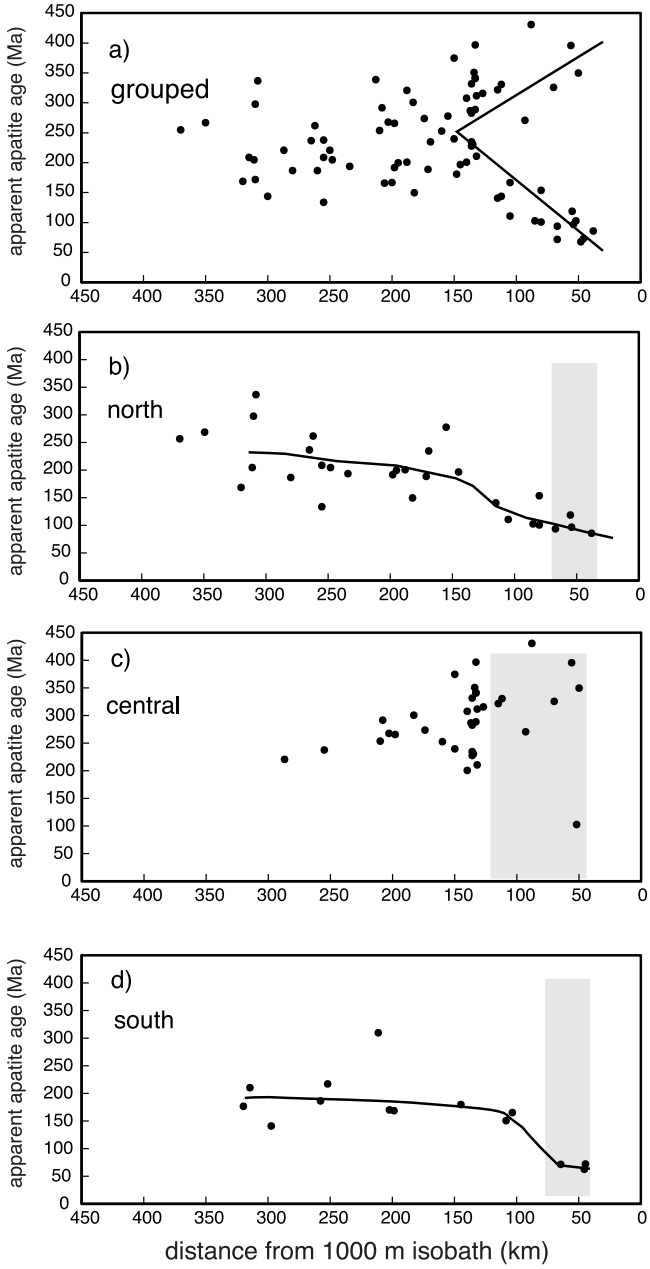

Figure 9. Apparent apatite age change with respect to the distance from the east coast 1000 m isobath. The shaded area represents the broad extent of the coastal plain.

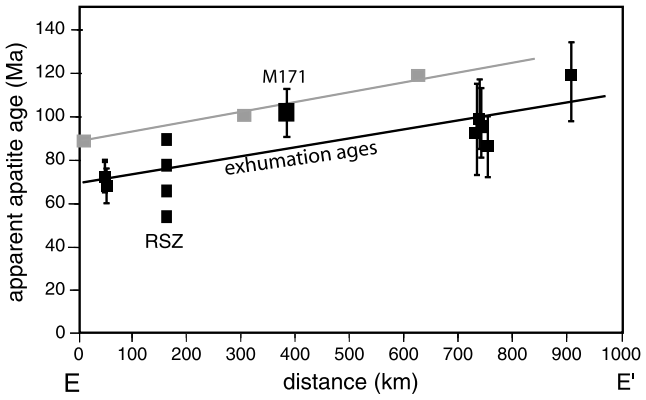

Figure 10. North-south variation in ages along the eastern coast margin (at altitudes less than 250 m) and excluding those Paleozoic ages of the central region. Errors are 2 sigma. Shaded boxes represent the time and position of Madagascar over the Marion hot spot after *Storey et al.* [1995] and *Torsvik et al.* [1998]. Line of section marked on Figure 4a.

but inspection of Landsat ETM+ images reveals a possible complex WNW-ESE trending system of minor faults. These may be the reason for the disrupted age-altitude pattern in Pic Boby. Nonetheless, a mean denudation rate of 7.5 m/Myr from 400 to 230 Ma can be made for this region.

[31] In an east-west profile from Brickaville to Antananarivo (Figures 3 and 8b) the age-altitude relationship indicates a break in slope between 115 and 110 Ma indicative of a renewed phase of cooling/exhumation. The older exhumation rate, from 190 to 115 Ma was about 6.5 m/Myr, almost identical to that of the Pic Boby region. This suggests that these two regions have undergone similar cooling histories from 400 until about 115Ma. The renewed rates beginning at about 115 Ma are an order of magnitude larger, approximately 62 m/Myr. It is possible that this phase was due to (1) the doming of the surface and enhanced exhumation at the time when this region lay above the Marion hot spot (Figure 2) in approximate agreement with the estimation of *Storey et al.* [1995] and *Torsvik et al.* [1998] and/or (2) that it could be due to resetting of the geotherms after the passage over the hot spot, and/or c) that this is the cooling associated with the rift shoulder exhumation with associated scarp retreat. It is difficult to distinguish between these possibilities due to the close relationship between the timing of rifting and hot spot position.

[32] No other regions or sites revealed simple relationships. This may be due to the fact that age-altitude relationships have been disturbed by the numerous faults that occur particularly on the western margin, many of them affecting Cretaceous sedimentary rocks along the west coast, with some as young as Neogene [*Piqué et al.*, 1999a] (Figure 5).

6.2. Distance From the 1000 m Isobath

[33] The western passive margin has clearly been modified through time with the deposition of sediments, faulting and some westward tilting [*Montenat et al.*, 1996]. In contrast, the eastern margin retains a coastal plain and a pronounced escarpment most likely related to the rifting from India-Seychelles. The relationship of the combined apatite ages to their distance from the 1000 m isobath (Figure 9a) is atypical compared to other passive margin studies (e.g., review by *Gunnell* [2000]), in which ages generally increase from the coast up and across the escarpment. In all published studies, inland plateaus, as expected, have the oldest ages which are unrelated to the rifting phase but represent some earlier phase of exhumation. In Madagascar, the youngest ages occur along the eastern coastal margin, but unusually, so also do some of the oldest (Figures 9a and 9c). The older group of ages all come from

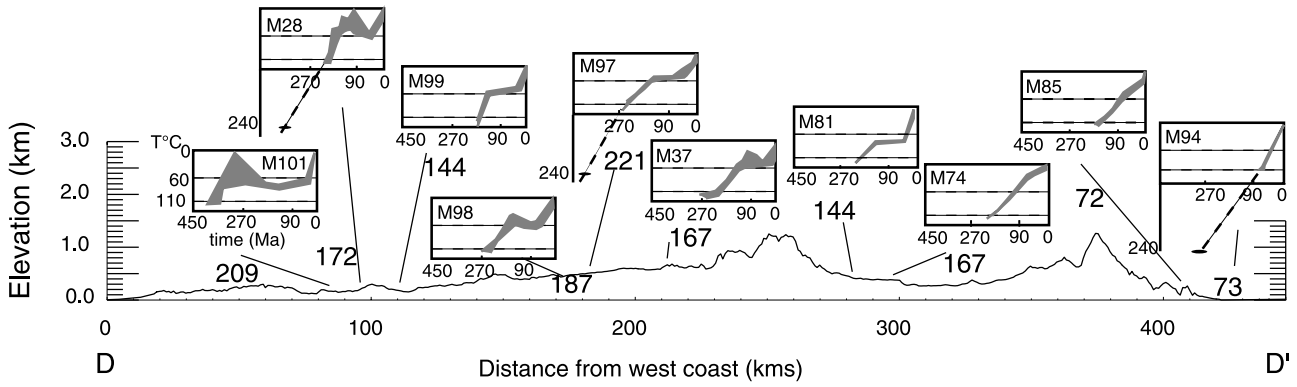

Figure 11. Representative thermal models for the region south of the RSZ along section D-D′ (Figure 4a). Large numbers are apparent apatite ages (Ma). Those with models extending to 240°C represent samples with zircon fission track ages (Figure 5 and Table 1). The topographic swath profile (25 km wide) was constructed by C. Duncan (University of Massachusetts) from GTOPO30 DEM data. Vertical exaggeration = 20.

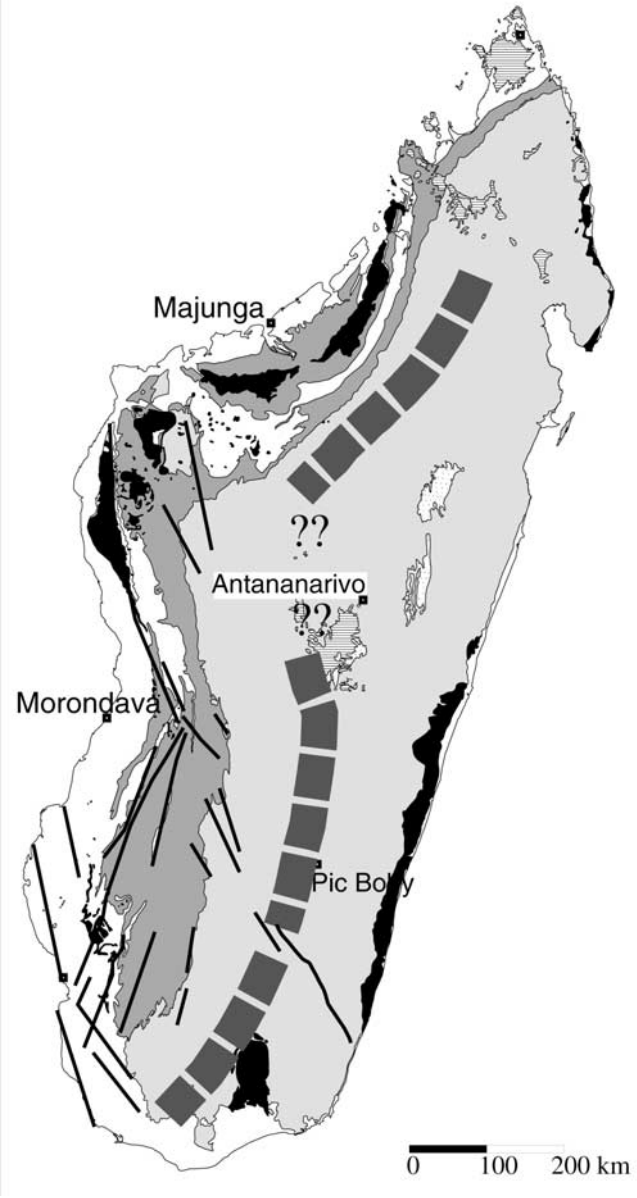

Figure 12. Suggested minimum eastern limits of the Jurassic-Cretaceous sedimentation on the western passive margin as shown by the heavy dashed line. Key for geology as in Figure 3.

the coastal plain region north of the RSZ and south of about latitude 20°S. This is consistent with the observation that the eastern central region, has remained stable probably at least since the Devonian. This region also has the widest coastal plain (Figure 9c) and is covered, often to the foothills, but not right up to the escarpment, by Late Cretaceous subaerial extrusives. The presence of these extrusives along the central eastern coast implies that there was here a coastal plain prior to the Cretaceous volcanism, most likely the floor of a rift which had developed before separation of the India-Seychelles plate. The rift was therefore formed before 88 Ma.

[34] Across the north and south segments of the east coast, a typical AFT pattern is revealed with the younger ages along the coastal margin increasing inland from the edge of the plain, (Figures 9b and 9d). In none of the regions is there any signature in the apparent ages themselves of the timing of rifting.

6.3. Hot Spot Trail Along the Eastern Margin?

[35] As mentioned above, the youngest apparent ages lie along the east coast margin with the exception of the central region. Excluding for the moment the central region, there is a younging trend from north to south of ages that lie at altitudes of <250 m (Figure 10).

[36] As discussed above, the ages westward from Brickaville have a break in slope between 115 and 110 Ma (Figure 8b) implying a renewed cooling event at about this time. This is marginally later than the position of the hot spot predicted by *Storey et al.* [1995] and *Torsvik et al.* [1998]. Thus the apparent apatite ages (101–86 Ma) most likely represent exhumation ages, due to erosion, perhaps after the passage of the hot spot. Further to the south in the region of Tôlañaro, ages are 73–68 Ma (Figure 5). *Storey et al.* [1995] predicted the position of the hot spot at the southern tip of Madagascar at 88 Ma. These ages may also represent exhumation after hot spot passage.

[37] In the central region, one age only along the coast is "young," M174 (103 Ma), and is surrounded by older ages (325–431 Ma). The question remains unanswered as to why only one site records a younger event. Similar mixtures of young and old ages were reported from the Indian west coastal margin by *Gunnell et al.* [2003], who found evidence of Deccan trap ages (65 Ma) scattered among much older ages. Because the central region of Madagascar has undergone very little erosion, this age more closely represents the actual timing of the position of the hot spot at this locality. As such it is again in agreement with the work of *Storey et al.* [1995] (Figure 10).

6.4. Thermal History

[38] Thermal modeling [*Gallagher*, 1995] has been applied to almost every sample analyzed. For simplicity, the variable paths will be discussed firstly within three regions - south, central and north. The thermal history in terms of burial, hence the limits of Mesozoic sedimentation onto the presently exposed basement, can be estimated.

6.4.1. Southern Region

[39] This region displays an extremely consistent pattern (Figure 11). The site closest to the Morondava basin margin, M101, reveals a cooling phase from Devonian to Permian. This initial cooling event may represent the rift shoulder exhumation during a period of Paleozoic intracontinental extension. It was followed by a phase of heating which certainly began somewhere between 270 and 200 Ma. The exact timing of the initiation of heating is not possible to ascertain because during this period the modeling is at temperatures less than 60°C where there can be little confidence in the predicted patterns. The heating event is assumed to be the result of burial by passive margin sediments; it lasted until middle Tertiary.

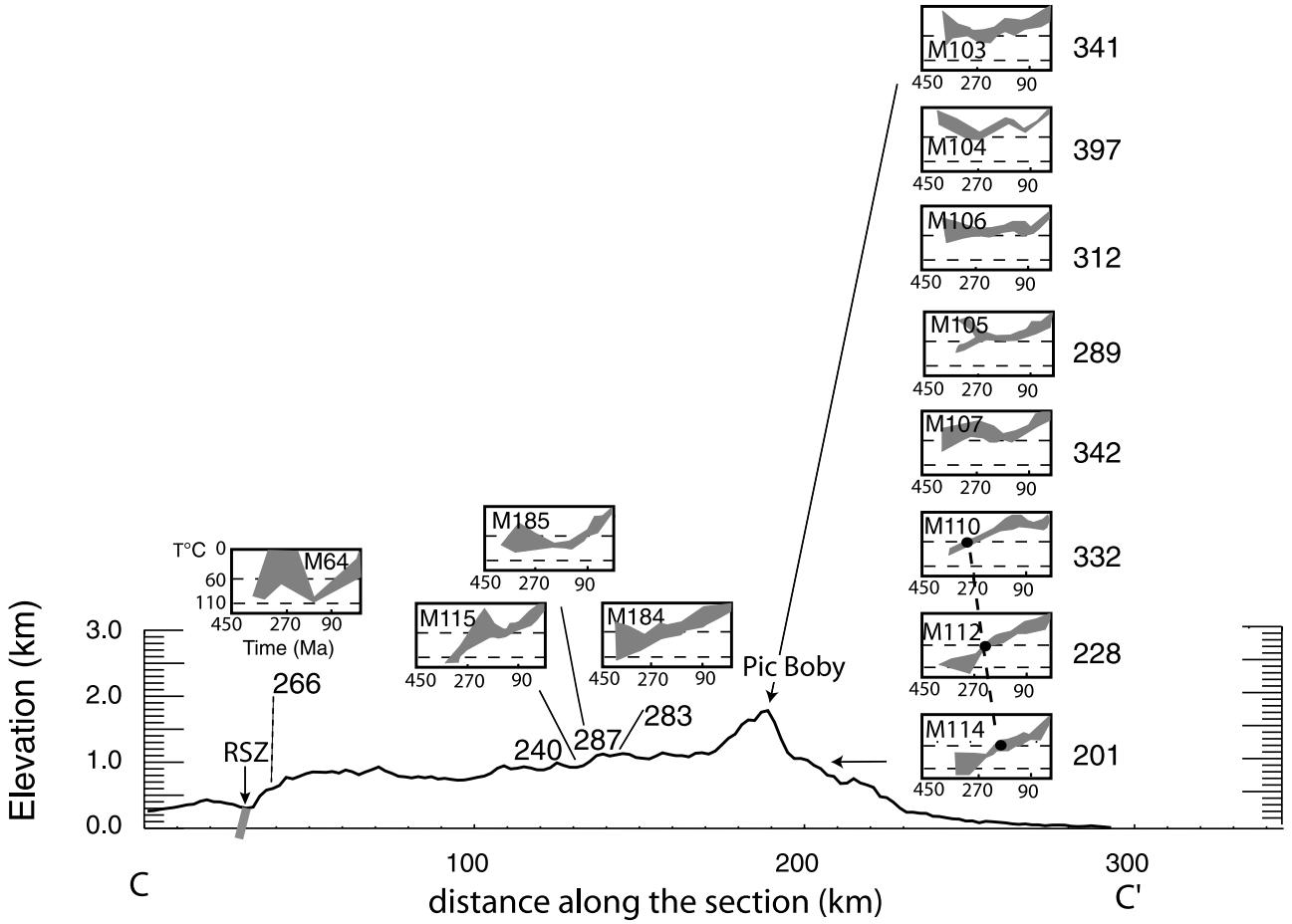

Figure 13. Representative thermal models across section, C-C′ from the southern central region of Madagascar. For section line see Figure 4a. Large numbers are apparent apatite ages (Ma). Site M115 has been projected south onto the line and site M64 has been projected northward. Sites M114 to M103 represent a vertical section through Pic Boby. The topographic swath profile (25 km wide) was constructed by C. Duncan (University of Massachusetts) from GTOPO30 DEM data. Vertical exaggeration = 20.

In order to determine the amount of burial the paleogeothermal gradient through time is required. However, since Madagascar has twice been in the structural position of a rift shoulder and had abundant Cretaceous volcanism, the gradient may have changed both temporally and spatially. Assuming a geothermal gradient of 20°C/km the amount of burial was less than 3 km. On the basis of the modeling, the limits of Jurassic and Cretaceous sedimentation which probably caused the heating event can be estimated using these cooling histories (Figure 12). Thus sedimentation extended further eastward than the present outcrop, overlying the presently exposed Precambrian basement.

[40] The first cooling phase becomes progressively younger in an easterly direction. Likewise, the subsequent heating phase youngs in an eastward direction with decreasing intensity and duration until along the eastern coastal sites only a long period of simple cooling is recognized. The zircon fission track age of 341 ± 76 Ma, sample M94 (Figures 5 and 11; Table 1) suggests that only simple monotonic cooling has taken place here over this time period. No temperature pulse that might be related to the passage of the hot spot is visible in any of the cooling patterns. Therefore, although the ages along the east coast margin coincide well with the trace of the Marion hot spot as supposed by *Storey et al.* [1995] and *Torsvik et al.* [1998], they may also be interpreted as the result of progressive exhumation of the uplifting rift shoulder related to the rifting between Madagascar and East Africa, which was coincident with the hot spot position.

6.4.2. Southern Central Region

[41] This region is dominated by apparent ages older than 200 Ma and very often older than 300 Ma, (barring sample M171). The samples from the western margin yield thermal histories (Figure 13) equivalent to those of the western margin of the southern region and are interpreted in the same manner. The eastern limit of sedimentation is close

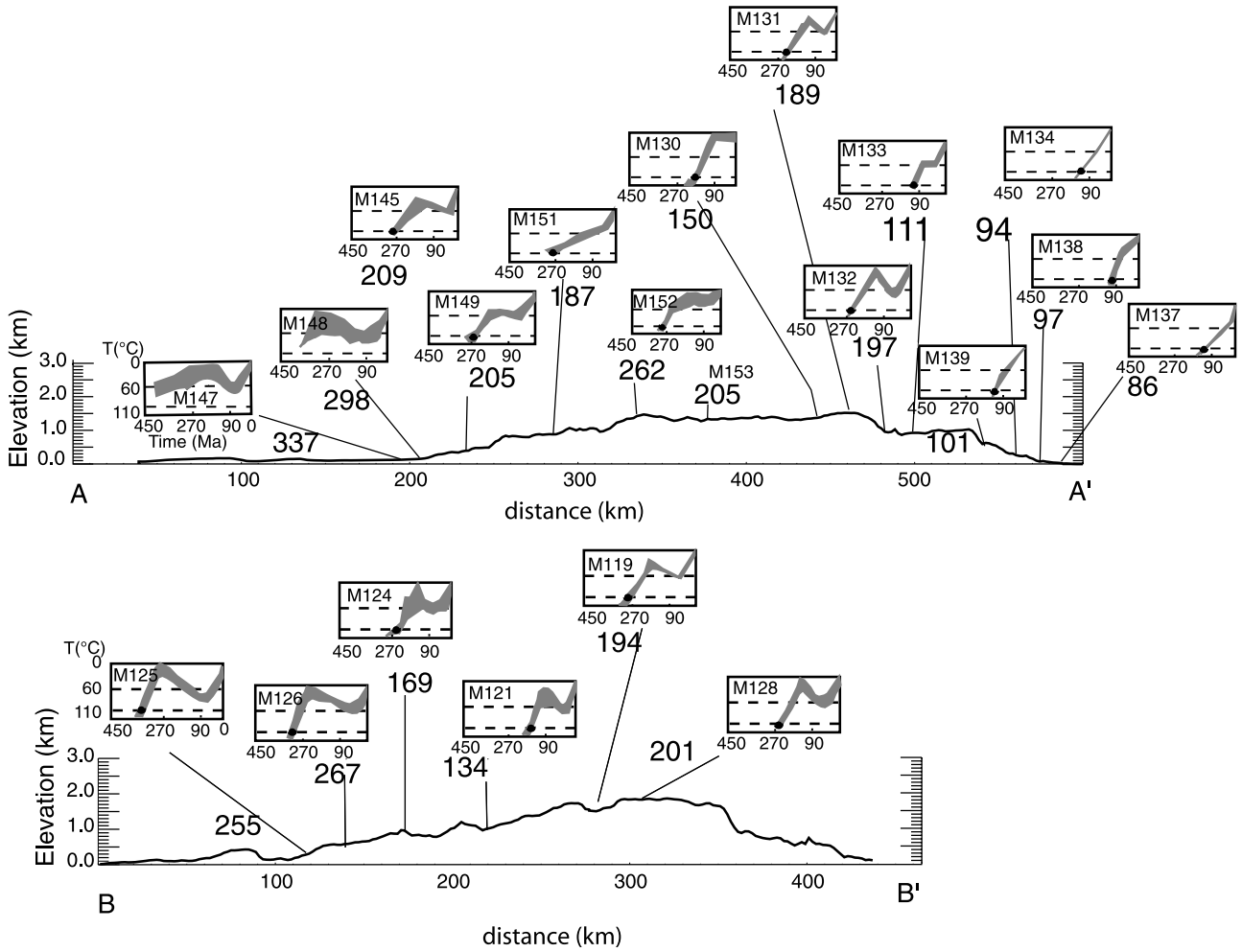

Figure 14. Representative thermal models for the northern region along sections A-A′ and B-B′. For section line see Figure 4a. Sample M145 does not lie on section A-A′, but to the north, but is included to emphasize the similarity of thermal histories along the western margin. The solid points represent the time at which the rocks passed into the partial annealing zone. The larger numbers are apparent apatite ages (Ma). The topographic swath profile (25 km wide) was constructed by C. Duncan (University of Massachusetts) from GTOPO30 DEM data. Vertical exaggeration = 20.

to site M184 where only simple monotonic cooling took place from at least Silurian time (Figure 13). At Pic Boby to the east, no disruption is revealed in the modeled data sets which point to a simple very slow monotonic pattern of cooling; there is no evidence that this region was ever heated. The upper sites have not seen temperatures greater than 60°C in the last 360 million years confirming extraordinarily low cooling rates. Assuming 3–4 km of material have been removed in the last 360 Ma, exhumation rates of 8–11 m/Myr are calculated which are in the same order of magnitude as the rates estimated from age-altitude relationships.

6.4.3. Northern Region (North of ~20°S)

[42] In this region (Figure 14), a pronounced west-east variation in cooling histories is best illustrated by cross sections, A-A′ and B-B′ (Figures 4a and 14). Along the western margin close to the present limits of the Morondava and Mahajanga Basins, samples M125, M126, M147 and M148 reveal a period of cooling (about 2°C/Ma) from at least middle Carboniferous through to middle Permian, a pattern similar to that at the western margin further south and the thermal history is thus interpreted in a similar manner. This cooling was followed by a heating event that lasted until about 90 Ma.

[43] Eastward (inland) of the above sites, the rocks did not cool (in general) to less than 60°C until after at least 180 Ma (e.g., M121, 124, 128, 145, 149). Shortly after this first cooling phase, they were reheated to a maximum of 70°C. This is coincident with the time of the beginning of sedimentation in the Mahajanga Basin [*Razafindrazaka et al.*, 1999]. Again, the position of the eastern margin of sedimentation lies eastward of the present outcrop (Figure 12).

[44] As in the other regions, initial exhumation was diachronous, the subsequent heating event diminishes east-

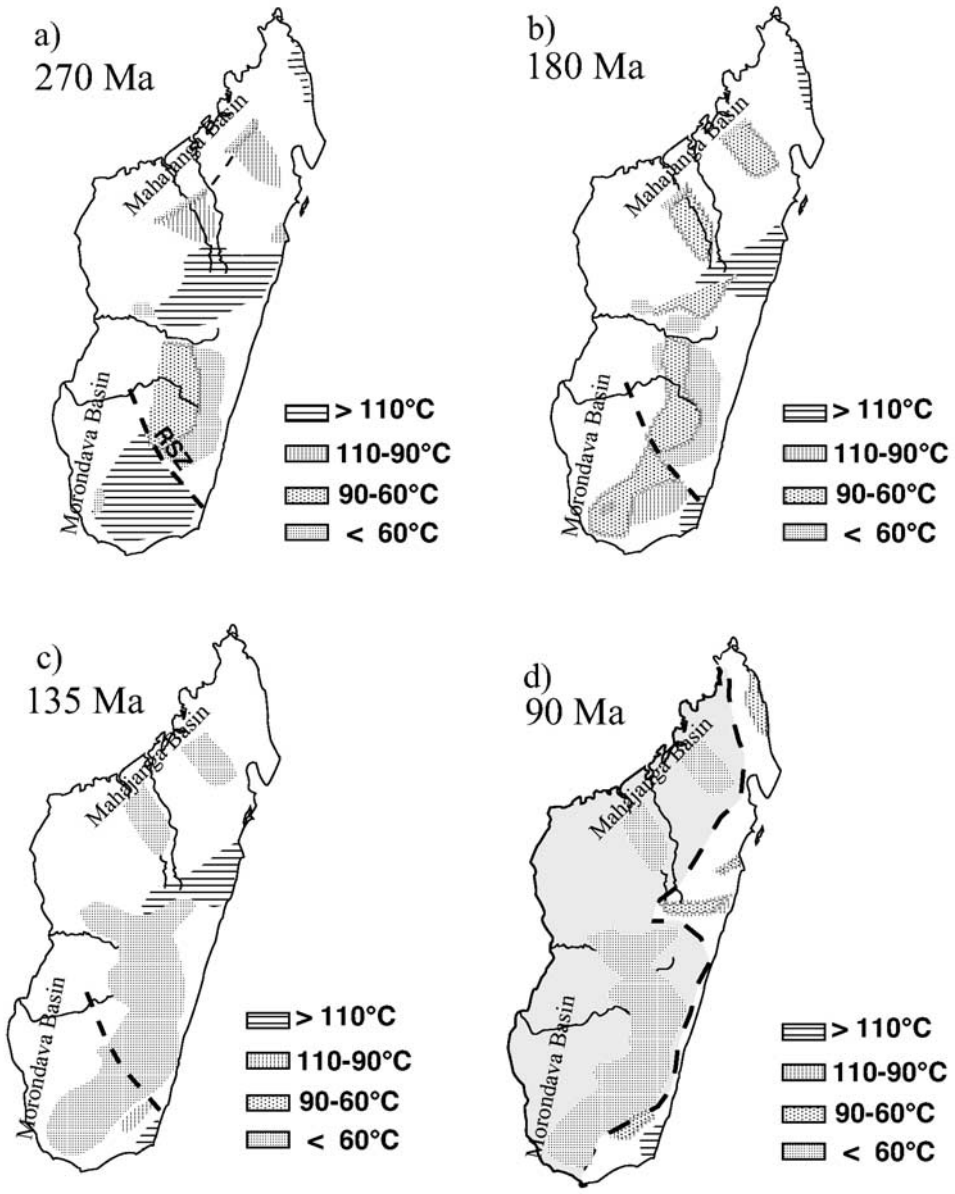

Figure 15. Temperature distribution through time. Temperatures taken from thermal models (Monte Trax [*Gallagher*, 1995]).

ward, until finally along the eastern coastal margin only simple monotonic cooling can be identified through FTA. A heat pulse from the Marion hot spot is not recognized in the thermal modeling but one cannot exclude the possibility that it may have only affected those rocks that were deeper such that it may only be identified in the zone of temperatures higher than 110°C.

6.4.4. Temperature Through Time

[45] Figure 15 illustrates the temperature of the different regions at specific times using data extracted from the Monte Trax models. It was decided not to run a contour procedure over the whole island because of the nonstatistical distribution of the sample sites, which could lead to a smoothing effect over large regions where data are missing, as well as the problems of altitude related discrepancies. Instead, regions that had a reasonable close sample density were separately treated.

[46] At 270 Ma the data presented in this way clearly again emphasize the different trends observed earlier (Figure 15a). The RSZ stands out clearly as a structure separating two regions with different temperatures at this time. South of the RSZ almost the whole region was at temperatures greater than 110°C. In the central region the eastern side was already at temperatures less than 60°C with an increase to 60°–90°C westward.

[47] At about 180 Ma (Figure 15b), the thermal structure of the region south of the RSZ was still distinct from that north of the fault. A temperature increase to the east is suggested from the data. Again this may point to the fact that at this time the western region was the margin of the

Morondava Basin and was an eastward tilted block whose western rim represented the uplifted shoulder. North of the RSZ a paleotemperature distribution similar to that at 270 Ma remains, with an increase in temperatures to the west but all less than 90°C. There is not a sharp clear boundary between the northern and central regions. Only a corridor of lower temperatures exists.

[48] By 135 Ma most of the basement was at temperatures less than 60°C (Figure 15c). The exceptions are along the eastern margin of the north and south regions. Implications are that the RSZ was no longer active with respect to the magnitude of vertical displacements that may be recorded through fission track analysis. However, the Neogene continental sediments [*Hottin*, 1976] immediately to the north of the Ranotsara Fault and the strongly deflected drainage pattern over the fault (Figure 4b) are suggestive of more recent activity. The abrupt closure of the southern limits of the Cretaceous extrusive volcanic suites at the RSZ is also suggestive of the fact that some uplift has been ongoing until some time after about 88 Ma. By 90 Ma, the temperature distribution had changed very little (Figure 15d). Clearly, the highest temperatures are recorded along the eastern margin except for those in the central region. This implies that cooling along the northern and southern eastern margin has been more rapid since approximately 90 Ma in order to exhume these rocks. A marked change to rapid cooling at about 115–110 Ma was identified already along the east coast inland from Brickaville. A westward tilting of the north and south regions of the island is implied, while the central region remained more stable.

6.4.5. Basin Formation

[49] Integrating our interpretations based on fission track analysis with the regional geology, the thermal history of the Precambrian basement of the island can be correlated with basin development. The Mahajanga Basin is delimited on its southwestern margin by a horst of basement and Paleozoic sediments [*Razafindrazaka et al.*, 1999]. From the thermal histories extracted from the fission track data sets there is a merging boundary at 180 Ma with this region and that to the south (Figure 15b). It is identified through a low-temperature (<60°C) corridor running WNW-SSE at approximately 20°S. Further south, the Bongolava-Ranotsara Shear Zone is considered to mark the northeastern structural boundary of the Morondava basin [*Piqué et al.*, 1999b; *Montenat et al.*, 1996]. The current fission track data set is consistent with this interpretation in that the thermal histories at 180 Ma are strongly contrasting across the Ranotsara Shear Zone. The eastern central region has been essentially stable, possibly behaving as a structural high since Devonian times. Hence, on the basis of the data from this study we suggest a refinement to Figure 11 of *Montenat et al.* [1996] (Figure 16) illustrating the development of the western marginal basins.

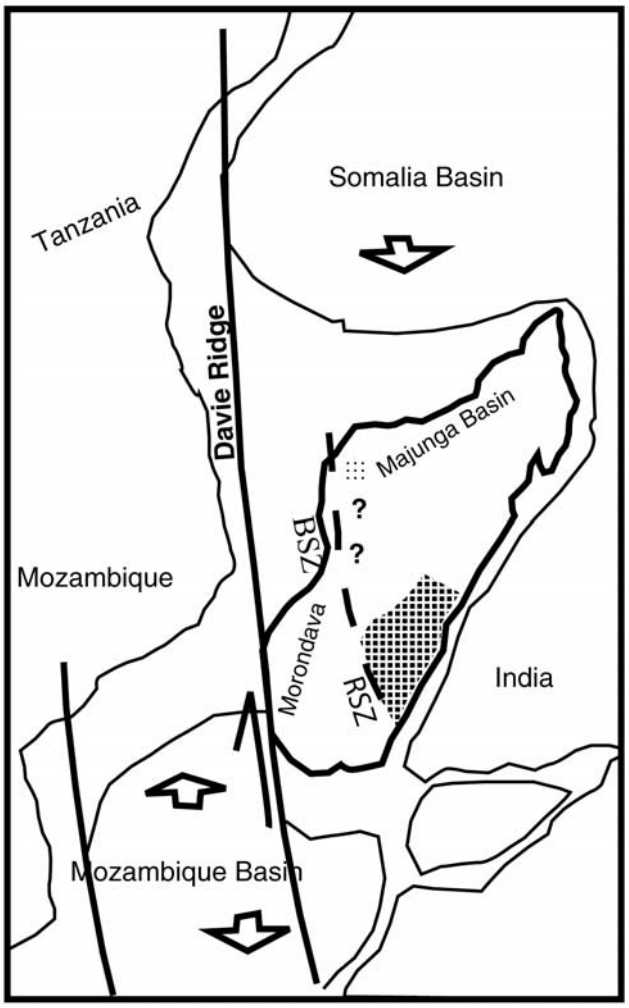

Figure 16. Schematic illustration (modified after *Montenat et al.* [1993, 1996]) of the structural control during the initiation of the Morandava and Majunga Basins. The shaded area represents the region of extreme stability since the Devonian. RSZ and BSZ represent respectively the Ranotsara and the Bongolava Shear Zones.

7. Conclusions

[50] The following points summarize our conclusions.

[51] 1. The fission track analysis reveals a thermochronological division of the island along both north-south and east-west lines. A southern region is clearly defined south of the RSZ. To the north of this shear zone, is a region of extreme thermal stability which passes northward into a zone with thermochronological parameters more similar to the southern region.

[52] In each of these regions there is an east-west variation. The northern and southern regions have a general younging trend in apparent apatite ages from west to east in contrast to the central zone where ages young from east to west.

[53] 2. The western samples of all regions yield thermal histories that involve episodes associated with Paleozoic cooling. This initial cooling along the western margins was most likely related to intracontinental rifting. This was followed by a heating phase which is interpreted as being due to burial by Mesozoic sediments associated with the

drifting phase and the formation of the western passive margin.

[54] 3. In the northern and southern regions, the first phase of cooling through 110°C in general began progressively later in an easterly direction. The subsequent heating phase also began progressively later eastward. This diachroneity is interpreted as progressive on-lap by late Paleozoic and Mesozoic sediments extending eastward onto the Precambrian basement rocks. The minimum eastward extension of the ocean can be estimated such that there was sedimentation at least as far as the central region of Madagascar with the implication that the island may have had subdued topography at that time.

[55] 4. The eastern margins of the northern and southern regions have undergone a simple cooling history with the rocks passing through the 110°C isotherm during the Cretaceous. That this is cooling related to the denudation of the uplifting margin during splitting from India-Seychelles or whether it is due to cooling after the passage of Madagascar over the Marion hot spot is open to conjecture at this point. The fact that the thermal models do not record any heating event at the time of the hot spot is a concern on one hand. Yet the apparent ages are coincident with the positions of the hot spot as postulated by *Storey et al.* [1995] and *Torsvik et al.* [1998]. Conversely, the monotonic cooling may simply be a reflection of the long term cooling related to progressive southward splitting of the island from India-Seychelles over approximately 30 Myr with related westward tilting and erosion of this margin.

[56] 5. A region of long-term tectonic stability characterizes the eastern central part of the island. It is delimited by the RSZ to the south and merges into the northern region at about latitude 20°S. This region has undergone excessively slow cooling with estimated exhumation rates of the order of 1–5 m/Myr since at least the Devonian. It is possible that this region may have formed the northern and southern margins of the Morondava and Mahajanga Basins, respectively.

[57] **Acknowledgments.** Roger Rambeloson (Université d'Antananarivo) is thanked for help in administrative matters, Rachel Razafimbelo for support in the field, and WWF Madagascar for providing access to the Andringitra National Park. We thank Claudio Mazzoli (University of Padova) for providing a series of samples from central Madagascar (MUP 120, 135, 103, 52, 188, 205, 209 and 211) and Alan Collins for three samples from northern Madagascar (M97/81, M97/148 and M97/111). This research was supported by the Swiss Academy of Natural Sciences, the ETH Zürich (grant 0-20-015-95) and the Natural Sciences and Engineering Research Council of Canada (grant RGPIN 227475-2000) to D. G., the Foundation Stichting Dr. Schürmannfonds (grant 1994/02), the Hochschulstiftung Bern (grant 64/95), the K. Bretscher Stiftung (Bern) and the Swiss National Science Fund (grants 2100-054112.98/1 and 2000-65306.01) to G. S. Giulio Viola is thanked for his comments on an earlier version of the manuscript. We appreciate very much the time put into reviewing by Alan Collins, Maarten de Wit, and an anonymous colleague.

References

Andriamarofahatra, J., H. de la Boisse, and C. Nicollet (1990), Datation U-Pb sur monazites et zircons du dernier épisode tectono-métamorphique granulitique majeur dans le Sud-Est de Madagascar, *C. R. Acad. Sci. Paris, Ser. II*, *310*, 1643–1648.

Bertil, D., and J. M. Regnoult (1998), Seismotectonics of Madagascar, *Tectonophysics*, *294*, 57–74.

Besairie, H. (1964), Madagascar: Carte géologique 1:1,000,000, Serv. Geol. Madagascar, Antananarivo.

Besairie, H. (1973), Précis de géologie malgache, *Ann. Geol. Madagascar*, *36*, 1–141.

Brandon, M. T., M. K. Roden-Tice, and J. I. Garver (1998), Late Cenozoic exhumation of the Cascadia accretionary wedge in the Olympic Mountains, northwest Washington State, *GSA Bull.*, *110*, 985–1009.

Brown, R. W., M. A. Summerfield, and A. J. W. Gleadow (1994), Apatite fission track analysis: Its potential for estimation of denudation rates and the assessment of models of long term landscape development, in *Process Models and Theoretical Geomorphology*, edited by M. J. Kirkby, pp. 23–53, John Wiley, Hoboken, N. J.

Burtner, R. L., A. Nigrini, and R. A. Donelick (1994), Thermochronology of the Lower Cretaceous source rocks in the Idaho-Wyoming Thrust Belt, *AAPG. Bull.*, *78*, 1613–1636.

Clark, D. N. (1998), Review of the exploration potential of Madagascar, *Houston Geol. Soc. Bull.*, *40*, 23–29.

Collins, A. S. (2000), The Tectonic Evolution of Madagascar: Its place in the East African Orogen, *Gondwana Res.*, *3*, 549–552.

Collins, A. S., and B. F. Windley (2002), The tectonic evolution of central and northern Madagascar and its place in the final assembly of Gondwana, *J. Geol.*, *110*, 325–339.

Collins, A. S., S. Johnson, I. C. W. Fitzsimons, C. McA. Powell, B. Hulscher, J. Abello, and T. Razakamanana (2003a), Neoproterozoic deformation in central Madagascar: A structural section through part of the East African Orogen, in *Proterozoic East Gondwana: Supercontinent Assembly and Breakup*, edited by M. Yoshida, B. Windley, and S. Dasgupta, *Geol. Soc. Spec. Publ.*, *206*, 381–399.

Collins, A. S., A. Kröner, I. C. W. Fitzsimons, and T. Razakamanana (2003b), Detrital footprint of the Mozambique Ocean: U-Pb SHRIMP and Pb evaporation zircon geochronology of metasedimentary gneisses in eastern Madagascar, *Tectonophysics*, *375*, 77–99.

Collins, A. S., I. C. W. Fitzsimons, B. Hulscher, and T. Razakamanana (2003c), Structure of the eastern margin of the East African Orogen in central Madagascar, *Precambrian Res.*, *123*, 111–133.

Corrigan, J. D. (1993), Apatite fission-track analysis of Oligocene strata in South Texas, U.S.A., *Chem. Geol.*, *104*, 227–249.

de Wit, M. J. (2003), Madagascar: Heads it's a continent, tails it's an island, *Annu. Rev. Earth Planet. Sci.*, *31*, 213–248.

de Wit, M. J., S. A. Bowring, L. D. Ashwal, L. G. Randrianasolo, V. P. I. Morel, and R. A. Rambeloson (2001), Age and tectonic evolution of Neoproterozoic ductile shear zones in southwestern Madagascar, with implications for Gondwana studies, *Tectonics*, *20*, 1–45.

Dumitru, T. A. (1995), A new computer automated microscope stage system for fission track analysis, *Nucl. Tracks Radiat. Meas.*, *21*, 575–580.

Eldholm, O., and A. Todal (1997), Indian continental margin and Deccan large igneous province, paper presented at International Lithosphere Program Workshop on Volcanic Margins, GeoForschungs-Zentrum Potsdam, Potsdam, Germany.

Emmel, B., J. Jacobs, G. Graser, and T. Razakamanana (2002), Exhumation history of central Madagascar: Evidence from apatite fission-track analysis, *Geotemas*, *4*, 72–73.

Fernandez, A., and G. Schreurs (2003), Tectonic evolution of the Proterozoic Itremo Group metasediments in central Madagascar, in *Proterozoic East Gondwana: Supercontinent Assembly and Breakup*, edited by M. Yoshida, B. Windley, and S. Dasgupta, *Spec. Publ. Geol. Soc.*, *206*, 381–399.

Fernandez, A., G. Schreurs, I. M. Villa, S. Huber, and M. Rakotondrazafy (2003), Age constraints on the tectonic evolution of the Itremo region in central Madagascar, *Precambrian Res.*, *123*, 87–110.

Galbraith, R. F., and G. M. Laslett (1993), Statistical models for mixed fission-track ages, *Nucl. Tracks Radiat. Meas.*, *21*, 459–470.

Gallagher, K. (1995), Evolving temperature histories from apatite fission-track data, *Earth Planet. Sci. Lett.*, *136*, 421–435.

Gallagher, K., C. J. Hawkesworth, and M. S. M. Mantovani (1995), Denudation, fission track analysis and long term evolution of passive margin topography: Application to the southeast Brazilian margin, *J. S. Am. Earth Sci.*, *8*, 65–77.

Gleadow, A. J. W., and I. Duddy (1981), A natural long term annealing experiment for apatite, *Nucl. Tracks Radiat. Meas.*, *5*, 169–174.

Goncalves, P., C. Nicollet, and J.-M. Lardeaux (2003), Finite strain pattern in Andriamena unit (north-central Madagascar): Evidence for late Neoproterozoic-Cambrian thrusting during continental convergence, *Precambrian. Res.*, *123*, 135–157.

Gradstein, F. M., F. P. Agterberg, J. G. Ogg, J. Hardenbol, P. van Veen, J. Thierry, and Z. Huang (1994), A Mesozoic timescale, *J. Geophys. Res.*, *99*, 24,051–24,074.

Green, P. F., I. R. Duddy, G. M. Laslett, K. A. Hargety, A. J. W. Gleadow, and J. F. Lovering (1989), Thermal annealing of fission-tracks in apatite; 4, Quantitative modelling techniques and extension to geological time scales, *Chem. Geol.*, *79*, 155–182.

Gunnell, Y. (2000), Apatite fission track thermochronology: An overview of its potential and limitations in geomorphology, *Basin Res.*, *12*, 115–132.

Gunnell, Y., and L. Fleitout (1998), Shoulder uplift of the western Ghats passive margin, India: A denudational model, *Earth Surf. Processes Landforms*, *23*, 391–404.

Gunnell, Y., K. Gallagher, A. Carter, M. Widdowson, and A. J. Hurford (2003), Denudation history of the continental margin of western peninsular India since the early Mesozoic—Reconciling apatite fission-track data with geomorphology, *Earth Planet. Sci. Lett.*, *215*, 187–201.

Handke, M., R. D. Tucker, and L. D. Ashwal (1999), Neoproterozoic continental arc magmatism in west-central Madagascar, *Geology*, *27*, 351–354.

Hottin, G. (1976), Présentation et essai d'interprétation du Précambrien de Madagascar, *Bull. Bur. Rech. Geol. Min. Fr., Sect. 2*, 117–153.

Hurford, A. J., and P. F. Green (1983), The zeta age calibration of fission-track dating, *Chem. Geol.*, *41*, 285–317.

Kröner, A., I. Braun, and P. Jaecker (1996), Zircon geochronology of anatectic melts and residues from a high-grade pelitic assemblage at Ihosy, southern Madagascar: Evidence for Pan-African granulite metamorphism, *Geol. Mag.*, *133*, 311–323.

Kröner, A., B. F. Windley, P. Jaeckel, T. S. Brewer, and T. Razakamanana (1999), Precambrian granites, gneisses and granulites from Madagascar: New zircon ages and regional significance for the evolution of the Pan-African orogen, *J. Geol. Soc. London*, *156*, 1125–1135.

Kröner, A., E. Hegner, A. S. Collins, B. F. Windley, T. S. Brewer, T. Razakamanana, and R. T. Pidgeon (2000), Age and magmatic history of the Antananarivo Block, central Madagascar, as derived from zircon geochronology and Nd isotopic systematics, *Am. J. Sci.*, *300*, 251–288.

Laslett, G. M., P. F. Green, I. R. Duddy, and A. J. W. Gleadow (1987), Thermal annealing of fission tracks in apatite; 2, A quantitative analysis, *Chem. Geol.*, *65*, 1–13.

Martelat, J. E., J. M. Lardeaux, C. Nicollet, and R. Rakotondrazafy (2000), Strain pattern and late Precambrian deformation history in southern Madagascar, *Precambrian Res.*, *102*, 1–20.

Meert, J. G. (2003), A synopsis of events related to the assembly of eastern Gondwana, *Tectonophysics*, *362*, 1–40.

Meert, J. G., C. M. Hall, A. Nédélec, and M. O. Madison Razanatseheno (2001), Cooling of a late-syn orogenic pluton: Evidence from laser K-feldspar modelling of the Carion Granite, Madagascar, *Gondwana Res.*, *4*, 541–550.

Montenat, C., R. Lalaoharijaona, and M. Croisile (1993), La séquence tectono-sédimentaire de la marge ouest-malgache au Jurassique (bassin de Morondava, Madagascar), *C. R. Acad. Sci., Ser. IIb Mec. Phys. Chim. Sci.*, *317*, 811–818.

Montenat, C., L. Ramahavory, and M. Croisile (1996), Tectonic and sedimentary evolution of the western Madagascan margin during Jurassic in the Morondava Basin, Madagascar, *Bull. Cent. Rech. Elf Explor. Prod.*, *20*, 323–340.

Nédélec, A., B. Ralison, J.-L. Bouchez, and V. Grégoire (2000), Structure and metamorphism of the granitic basement around Antananarivo: A key to the Pan-African history of central Madagascar and its Gondwana connections, *Tectonics*, *19*, 997–1020.

Nichols, G. J., and M. C. Daly (1989), Sedimentation in an intracratonic extensional basin: The Karoo of the Central Morondava Basin, Madagascar, *Geol. Mag.*, *126*, 339–354.

Nicollet, C. (1990), Crustal evolution of the granulites of Madagascar, in *Granulites and Crustal Evolution*, vol. 311, *NATO ASI Ser., Ser. C Math. Phys. Sci.*, edited by D. Vielzeuf and P. Vidal, pp. 291–310, Kluwer Acad., Norwell, Mass.

O'Sullivan, P. B., and R. R. Parrish (1995), The importance of apatite composition and single-grain ages when interpreting fission track data from plutonic rocks: A case study from the Coast Ranges, British Columbia, *Earth Planet. Sci. Lett.*, *132*, 213–224.

Paquette, J. L., and A. Nédélec (1998), A new insight into Pan-African tectonics in the East-West Gondwana collision by U-Pb zircon dating of granites from central Madagascar, *Earth Planet. Sci. Lett.*, *155*, 45–56.

Paquette, J. L., A. Nédélec, B. Moine, and M. Rakotondrazafy (1994), U-Pb, single zircon Pb-evaporation, and Sm-Nd isotopic study of a granulite domain in SE Madagascar, *J. Geol.*, *102*, 523–538.

Paquette, J.-L., B. Moine, and M. Rakotondrazafy (2003), ID-TIMS using the step-wise dissolution technique versus ion microprobe U-Pb dating of metamict Archean zircons from NE Madagascar, *Precambrian Res.*, *121*, 73–84.

Piqué, A., E. Laville, P. Chotin, J. Chorowicz, S. A. Rakotondraompiana, and C. Thouin (1999a), L'extension à Madagascar du Néogène à l'actuel: Arguments structuraux et géophysiques, *J. Afr. Earth Sci. Middle East*, *28*, 975–983.

Piqué, A., E. Laville, G. Bignot, M. Rabarimanana, and C. Thouin (1999b), L'ouverture et le développement du basin de Morandava (Madagascar) du Carbonifère supérieur au Jurassique moyen: Données stratigraphiques, sédimentaires, paléontologiques et structurales, *J. Afr. Earth Sci. Middle East*, *28*, 931–948.

Plummer, P. S. (1996), The Amirante Ridge/trough complex: Response to rotational transform rift/drift between Seychelles and Madagascar, *Terra Nova*, *8*, 34–47.

Rakotondraompiana, S. A., Y. Albouy, and A. Piqué (1999), Modèle de lithosphère pour l'île de Madagascar (Océan Indien occidental): Nouvelle interprétation des données gravimétriques, *J. Afr. Earth Sci. Middle East*, *28*, 961–973.

Rambolamanana, G., P. Suhadolc, and G. F. Panza (1997), Simultaneous inversion of hypocentral parameters and structure velocity of the central region of Madagascar as a premise for the mitigation of seismic hazard in Antananarivo, *Pure Appl. Geophys.*, *149*(4), 707–730.

Razafindrazaka, Y., T. Randriamananjara, A. Piqué, C. Thouin, E. Laville, J. Malod, and J.-P. Réhault (1999), Extension et sédimentation au Paléozoïque terminal et au Mésozoïque dans le bassin de Majunga (Nord-Ouest de Madagascar), *J. Afr. Earth Sci. Middle East*, *28*, 949–959.

Reeves, C., and M. J. de Wit (2000), Making ends meet in Gondwana: Retracing the transforms of the Indian Ocean and reconnecting continental shear zones, *Terra Nova*, *12*, 272–280.

Reeves, C. V., B. K. Sahu, and M. de Wit (2002), A re-examination of the paleo-position of Africa's eastern neighbours in Gondwana, *J. Afr. Earth Sci.*, *34*, 101–108.

Ségoufin, J., and P. Patriat (1980), Existence d'anomalies magnétiques mésozoïques dans le bassin de Somalie: Implications pour les relations Afrique-Antarctique-Madagascar, *C. R. Acad. Sci. Paris*, *291*, 85–88.

Seward, D. (1989), Cenozoic basin histories determined by fission-track dating of basement granites, South Island, New Zealand, *Chem. Geol.*, *79*, 31–48.

Seward, D., D. Grujic, and G. Schreurs (1998), The exhumation history of the East Madagascar continental margin: Inferences from apatite fission-track analysis, *J. Afr. Earth Sci.*, *27*, 176–178.

Seward, D., D. Grujic, and G. Schreurs (1999), Exhumation history of southern Madagascar as revealed by zircon and apatite fission-track thermochronology, *Gondwana Res.*, *2*, 353–354.

Seward, D., D. Grujic, and G. Schreurs (2000a), Post Pan-African events in Madagascar: Inferences from apatite fission-track analysis, in *Fission Track 2000: 9th International Conference on Fission Track Dating and Thermochronology*, *Abstracts*, vol. 58, pp. 289–290, Geol. Soc. of Austr., Sydney, N. S. W., Australia.

Seward, D., R. Spikings, G. Viola, A. Kounov, G. Ruiz, and N. Naeser (2000b), Etch times and operator variation for spontaneous track length measurements in apatites: An intra-laboratory check, *On Track*, *10*, 19–21.

Simpson, E. S. W., J. G. Sclater, B. Parsons, I. Norton, and L. Meinke (1979), Mesozoic magnetic lineations in the Mozambique basin, *Earth Planet. Sci. Lett.*, *43*, 260–264.

Storey, M., J. J. Mahoney, A. D. Saunders, R. A. Duncan, S. P. Kelley, and M. F. Coffin (1995), Timing of hot spot-related volcanism and the breakup of Madagascar and India, *Science*, *267*, 852–855.

Torsvik, T. H., R. D. Tucker, L. D. Ashwal, E. A. Eide, and N. A. Rakotosolofo (1998), Late Cretaceous magmatism in Madagascar: Palaeomagnetic evidence for a stationary Marion hot spot, *Earth Planet. Sci. Lett.*, *164*, 221–232.

Torsvik, T. H., R. D. Tucker, L. D. Ashwal, L. M. Carter, B. Jamtveit, K. T. Vidyadharan, and P. Venkataramana (2000), Late Cretaceous India-Madagascar fit and timing of break-up related magmatism, *Terra Nova*, *12*, 220–225.

Tucker, R. D., L. D. Ashwal, M. J. Handke, M. A. Hamilton, M. Le Grange, and R. A. Rambeloson (1999), U-Pb geochronology and isotope geochemistry of the Archean and Proterozoic rocks of north-central Madagascar, *J. Geol.*, *107*, 135–153.

United Nations Educational, Scientific, and Cultural Organization (1990), International geological map of Africa, scale 1:5,000,000, sheet 6, CGMW/UNESCO, Paris.

Valsangkar, A. B., C. Radhakrishnamurty, K. V. Subbarao, and R. D. Beckinsale (1981), Palaeomagnetism and potassium-argon age studies of acid igneous rocks from the St. Mary Islands, *Mem. Geol. Soc. India*, *3*, 265–276.

Wescott, W. A., and J. N. Diggins (1998), Depositional history and stratigraphical evolution of the Sakamena Group (Middle Karoo Supergroup) in the Morondava basin, Madagascar, *J. Afr. Earth Sci.*, *27*, 461–479.

Windley, B. F., A. Razafiniparany, T. Razakamanana, and D. Ackermand (1994), Tectonic framework of the Precambrian of Madagascar and its Gondwana connections: A review and reappraisal, *Geol. Rundsch.*, *83*, 642–659.

Yamada, R., T. Tagami, S. Nishimura, and H. Ito (1995), Annealing kinetics of fission tracks in zircon: An experimental study, *Chem. Geol.*, *122*, 249–258.

D. Grujic, Department of Earth Sciences, Dalhousie University, Halifax, N. S., Canada B3H 3J5.

G. Schreurs, Institute of Geological Sciences, University of Bern, CH-3012 Bern, Switzerland.

D. Seward, Geological Institute, Eidgenossische Technische Hochschule, Zurich, CH-8092 Zürich, Switzerland.